

# **TRANSIENT THERMOELASTIC ANALYSIS OF DISK BRAKE USING ANSYS SOFTWARE**

*A thesis*

*Submitted in partial fulfillment of the requirements for the award of*

*Degree of*

**MASTER OF ENGINEERING**

**IN**

***CAD/CAM & ROBOTICS ENGINEERING***

**Submitted By**

**RAJESH KUMAR**

**ROLL NO. 80681017**

*Under the guidance of*

**Dr. Vijay Kumar Jadon**

**Associate Professor**



**MECHANICAL ENGINEERING DEPARTMENT**

**THAPAR UNIVERSITY**

**PATIALA -147004, INDIA**

**JUNE, 2008**

# CERTIFICATE

This is to certify that the thesis entitled, “**Transient Thermo Elastic Analysis of Disk Brake Using ANSYS software**” is being submitted by Mr. Rajesh Kumar, in partial fulfillment of the requirements for the award of degree of Master of Engineering (Cad/Cam & Robotics Engineering) at Thapar University, Patiala. This is a record of student’s own work and carried out by him under my guidance and supervision. The matter is of desired standards for the award of the degree mentioned above.

**(Dr. Vijay Kumar Jadon)**

Associate Professor,  
Department of Mechanical Engg  
Thapar University  
Patiala -147004

**(Dr. S.K. Mohapatra)**

Professor & Head,  
Department of Mechanical Engg.  
Thapar University  
Patiala -147004

**(Dr. R.K. Sharma)**

Dean of Academic Affairs  
Thapar University  
Patiala -147004

# ACKNOWLEDGEMENTS

Words are often less to reveal one's deep regards. With an understanding that works like this can never be the outcome of a single person, I take this opportunity to express my profound sense of gratitude and respect to all those who helped me through the duration of this work.

I acknowledge with gratitude and humility to **Dr. Vijay Kumar Jadon** Associate Professor, Mechanical Engineering Department, Thapar University, Patiala for his valuable guidance, proper advice, painstaking and constant encouragement, which helped me to bring this present work to this level. His cooperation, experience and deep insight into the subject has not only improved my vision in this field but quality of this work also.

I also take pride of myself being son of ideal parents for their everlasting desire, sacrifice, affectionate blessings, care and support nothing would have been possible.

**Rajesh Kumar**

**(Roll No. 80681017)**

**M.E. (CAD/CAM & Robotics)**

# CONTENTS

	<b>Page No.</b>
CERTIFICATE	i
ACKNOWLEDGEMENT	ii
CONTENTS	iii
LIST OF FIGURES AND TABLES	v
ABSTRACT	x
<b>CHAPTER 1: INTRODUCTION</b>	<b>1-4</b>
1.1 Introduction	1
1.2 Classification of brakes	1
1.3 Disk brake	2
1.3.1 Swinging caliper disc brake	3
1.3.2 Sliding caliper disk brake	3
1.4 Problems in Disk brake	3
1.5 Objective of the present study	4
<b>CHAPTER 2: LITERATURE REVIEW</b>	<b>5-15</b>
<b>CHAPTER 3: FINITE ELEMENT ANALYSIS</b>	<b>16-30</b>
3.1 Introduction	16
3.2 Procedure for ANSYS analysis	16
3.2.1 Build the model	17
3.2.2 Material properties	17
3.2.3 Solution	17
3.3 Finite element formulations for heat conduction	22
3.4 Finite element formulation for elastic problem	23
3.5 Contact model for disk brake	24
3.6 Finite element model of disk brake	26
3.7 Transient thermo elastic analysis	28

3.7.1	Thermal analysis	28
3.7.2	Structural analysis	29
<b>CHAPTER 4: MODELING AND ANALYSIS</b>		<b>31-39</b>
4.1	Definition of problem domain	32
4.2	Dimensions of Disk brake	32
4.3	Finite element mesh	33
4.4	SOLID90 element geometry	35
4.5	Boundary conditions	36
4.5.1	Thermal boundary conditions	37
4.5.2	Structural Boundary condition	38
4.6	Solution	38
<b>CHAPTER 5: RESULTS AND DISCUSSION</b>		<b>40-61</b>
5.1	Validation of results	40
5.2	Thermo elastic behavior in repeated brake application	42
<b>CHAPTER 6: CONCLUSIONS</b>		<b>62-63</b>
<b>SCOPE FOR FURTHER STUDY</b>		<b>64</b>
<b>REFERENCES</b>		<b>65-66</b>

# LIST OF FIGURES AND TABLES

## List of Figures

Fig No.	Description	Page No
1.1	Disk Brake assembly	2
3.1	Contact models for elastic and heat conduction problem	25
3.2	Elastic finite element model for the transient thermo elastic analysis	27
3.3	Elastic finite element model for the transient thermo elastic analysis	27
4.1	Model of 24mm Disk Brake	32
4.2	Dimension of 24mm Disk Brake	33
4.3	Dimension of 12mm Disk Brake	34
4.4	Model of 12mm Disk Brake	34
4.5	Solid element geometry	35
4.6	Meshed 3-D model	36
4.7	Thermal model of Disk Brake	37
4.8	Structural model of Disk Brake	38
5.1	Load Curve	41
5.2	Heat Flux distribution on friction surfaces in various braking step	42
5.3	Temperature distribution on friction surfaces in various braking step	44
5.4	Heat Flux distribution on friction surfaces in various braking step	45
5.5	Heat Flux distribution on friction surfaces in various braking step	45
5.6	Heat Flux distribution on friction surfaces in various braking step	46
5.7	Heat Flux distribution on friction surfaces in various braking step	46

Fig No.	Description	Page No
5.8	Temperature distribution on friction surfaces in various braking step	47
5.9	Temperature distribution on friction surfaces in various braking step	49
5.10	Temperature distribution on friction surfaces in various braking step	49
5.11	Temperature distribution on friction surfaces in various braking step	50
5.12	Heat Flux distribution on friction surfaces in various braking step	51
5.13	Heat Flux distribution on friction surfaces in various braking step	51
5.14	Temperature distribution on friction surfaces in various braking step	52
5.15	Temperature distribution on friction surfaces in various braking step	52
5.16	Temperature distribution on friction surfaces in various braking step	53
5.17	Temperature contours of 24mm Cast Iron Disk (a)-(d)	54
5.18	Temperature contours of 24mm Stainless Steel Disk (a)-(d)	54
5.19	Temperature contours of 16mm Cast Iron Disk (a)-(d)	55
5.20	Temperature contours of 16mm Stainless Steel Disk (a)-(d)	55
5.21	Distribution of Von misses Stress in 24 mm Cast iron Disk	56
5.22	Distribution of Hoop Stress in 24 mm Cast iron Disk	56
5.23	Distribution of Von misses Stress in 24 mm Stainless Steel Disk	57
5.24	Distribution of Hoop Stress in 24 mm Stainless Steel Disk	57
5.25	Distribution of Von misses Stress in 16 mm Cast iron Disk	58
5.26	Distribution of Hoop Stress in 16 mm Cast iron Disk	58
5.27	Distribution of Von misses Stress in 16 mm Stainless Steel Disk	59
5.28	Distribution of Hoop Stress in 16 mm Stainless Steel Disk	59
5.29	Average displacement in 24 mm Cast Iron Disk	60

Fig No.	Description	Page No
5.31	Average displacement in 16 mm Cast Iron Disk	61
5.32	Average displacement in 16mm Stainless Steel Disk	61

## List of Tables

Table No.	Description	Page No
3.1	Description of step used in ANSYS	18
5.1	Material properties for Isotropic material	40
5.2	Material properties for Cast Iron Disk	43
5.3	Material properties for Stainless Steel Disk	44
5.4	Material properties for Orthotropic material	48
6.5	Conclusions	63

# NOMENCLATURE

$c$	Specific heat (J/kg K)
$C$	Capacity matrix
$D$	Elasticity matrix
$E$	Young's modulus (N/mm <sup>2</sup> )
$h$	Heat convection coefficient (W/m <sup>2</sup> K)
$k$	Thermal conductivity (W/m K)
$K$	Stiffness matrix
$K$	Conductivity matrix
$P$	Normal pressure (N/mm <sup>2</sup> )
$P$	Force vector
$P_h$	Hydraulic pressure (N/mm <sup>2</sup> )
$q$	Heat flux (W/m <sup>2</sup> )
$r, \theta, z$	Cylindrical coordinates
$R$	Heat source vector
$T$	Temperature (K)
$T_\infty$	Ambient temperature (K)
$U$	Displacement vector normal component of displacements
$\alpha$	Thermal expansion coefficient ( /°C)
$\epsilon$	Strain vector
$\mu$	Coefficient of friction
$\nu$	Poisson's ratio
$\rho$	Density (Kg/m <sup>3</sup> )
$\sigma$	Stress vector
$\omega$	Angular velocity (rad/s)

## Subscripts

$f$	Body force
$i, j$	Sub regions $i$ and $j$ , respectively
$n$	Normal direction surface traction
$\Delta t$	Temperature rise (K)

## **ABSTRACT**

A transient analysis for the thermo elastic contact problem of the disk brakes with heat generation is performed using the finite element analysis. To analyze the thermo elastic phenomenon occurring in the disk brakes, the occupied heat conduction and elastic equations are solved with contact problems.

The numerical simulation for the thermo elastic behavior of disk brake is obtained in the repeated brake condition. The computational results are presented for the distribution of heat flux and temperature on each friction surface between the contacting bodies. Also, thermo elastic instability (TIE) phenomenon (the unstable growth of contact pressure and temperature) is investigated in the present study, and the influence of the material properties on the thermo elastic behaviors (the maximum temperature on the friction surfaces) is investigated to facilitate the conceptual design of the disk brake system. Based on these numerical results, the thermo elastic behaviors of the carbon-carbon composites with excellent mechanical properties are also discussed.

# CHAPTER - 1

## INTRODUCTION

### 1.1 INTRODUCTION

A brake is a device by means of which artificial frictional resistance is applied to moving machine member, in order to stop the motion of a machine.

In the process of performing this function, the brakes absorb either kinetic energy of the moving member or the potential energy given up by objects being lowered by hoists, elevators etc. The energy absorbed by brakes is dissipated in the form of heat. This heat is dissipated in the surrounding atmosphere to stop the vehicle, so the brake system should have following requirements:

- The brakes must be strong enough to stop the vehicle with in a minimum distance in an emergency.
- The driver must have proper control over the vehicle during braking and vehicle must not skid.
- The brakes must have well anti fade characteristics i.e. their effectiveness should not decrease with constant prolonged application.
- The brakes should have good anti wear properties.

### 1.2 CLASSIFICATION OF BRAKES

The mechanical brakes according to the direction of acting force may be divided into the following two groups:

- Radial Brake
- Axial Brake

#### **Radial brakes:**

In these brakes the force acting on the brakes drum is in radial direction. The radial brakes may be subdivided into external brakes and internal brakes.

### **Axial Brakes:**

In these brakes the force acting on the brake drum is only in the axial direction. i.e. Disk brakes, Cone brakes.

### **1.3 DISK BRAKE**

A disk brake consists of a cast iron disk bolted to the wheel hub and a stationary housing called caliper. The caliper is connected to some stationary part of the vehicle like the axle casing or the stub axle as is cast in two parts each part containing a piston. In between each piston and the disk there is a friction pad held in position by retaining pins, spring plates etc. passages are drilled in the caliper for the fluid to enter or leave each housing. The passages are also connected to another one for bleeding. Each cylinder contains rubber-sealing ring between the cylinder and piston. A schematic diagram is shown in the figure 1.1.

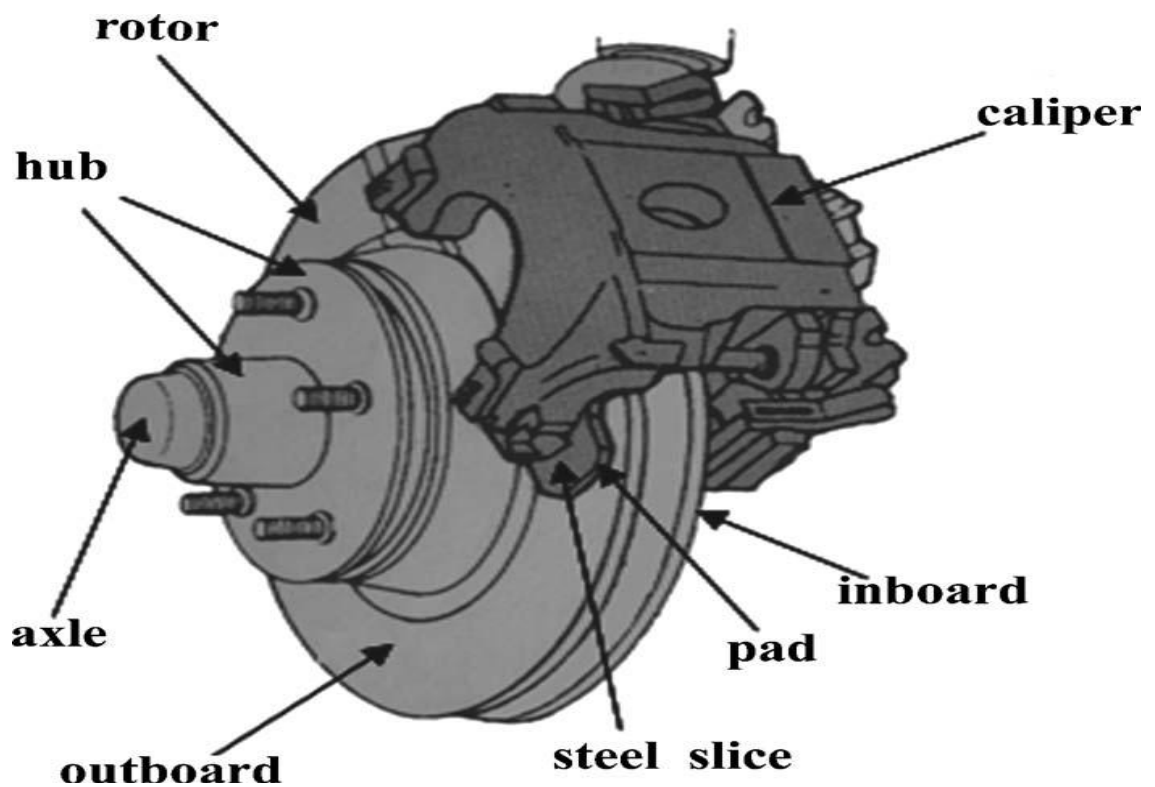


Fig 1.1 Disk Brake

The main components of the disc brake are:

- The **Brake Pads**
- The **Caliper** which contains the piston
- The **Rotor**, which is mounted to the hub

When the brakes are applied, hydraulically actuated pistons move the friction pads in to contact with the rotating disk, applying equal and opposite forces on the disk. Due to the friction in between disk and pad surfaces, the kinetic energy of the rotating wheel is converted into heat, by which vehicle is to stop after a certain distance. On releasing the brakes the rubber-sealing ring acts as return spring and retract the pistons and the friction pads away from the disk.

### **1.3.1 Swinging caliper disc brake:**

The caliper is hinged about a fulcrum pin and one of the friction pads is fixed to the caliper. The fluid under pressure presses the other pad against the disc to apply the brake. The reaction on the caliper causes it to move the fixed pad inward slightly applying equal pressure to the other side of the pads. The caliper automatically adjusts its position by swinging about the pin.

### **1.3.2 Sliding caliper disc brake:**

These are two pistons between which the fluid under pressure is sent which presses one friction pad directly on to the disc where as the other pad is pressed indirectly via the caliper.

## **1.4 PROBLEMS IN DISK BRAKE**

In the course of brake operation, frictional heat is dissipated mostly into pads and a disk, and an occasional uneven temperature distribution on the components could induce severe thermo elastic distortion of the disk. The thermal distortion of a normally flat surface into a highly deformed state, called thermo elastic transition. It sometimes occurs in a sequence of stable continuously related states as operating conditions change. At other

times, however, the stable evolution behavior of the sliding system crosses a threshold whereupon a sudden change of contact conditions occurs as the result of instability.

This invokes a feedback loop that comprises the localized elevation of frictional heating, the resultant localized bulging, a localized pressure increases as the result of bulging, and further elevation of frictional heating as the result of the pressure increase. When this process leads to an accelerated change of contact pressure distribution, the unexpected hot roughness of thermal distortion may grow unstably under some conditions, resulting in local hot spots and leaving thermal cracks on the disk. This is known as thermo elastic instability (TEI).

The thermo elastic instability phenomenon occurs more easily as the rotating speed of the disk increases. This region where the contact load is concentrated reaches very high temperatures, which cause deterioration in braking performance. Moreover, in the course of their presence on the disk, the passage of thermally distorted hot spots moving under the brake pads causes low-frequency brake vibration.

## **1.5 OBJECTIVE OF THE PRESENT STUDY**

The present investigation is aimed to study:

1. The given disk brake rotor of its stability and rigidity (for this Thermal analysis and coupled structural analysis is carried out on a given disk brake rotor.
2. Best combination of parameters of disk brake rotor like Flange width, Wall thickness and material there by a best combination is suggested.

# CHAPTER - 2

## LITERATURE REVIEW

In order to study the transient thermo elastic behavior of the disk brake , the literature related to the thermo elastic analysis of clutch, two sliding surfaces and brakes have been studied. Since in the past most of the studies of brake and clutch is carried out for thermo elastic analysis by considering it as a case of two dimensional. The following section details the literature available and relevant to the proposed study of transient thermo elastic analysis of a solid disk brake, as a case of three dimensional.

**F.E. Kennedy et al [1]** developed the numerical and experimental methods applied to tribology. He improved the techniques for Finite Element Analysis of sliding surface temperature. Essential component of manually operated vehicle transmissions is the synchronizer. Synchronizers have the task of minimizing the speed difference between the shifted gearwheel and the shaft by means of frictional torque before engaging the gear. Proper operation requires a sufficiently high coefficient of friction. It is common practice to investigate the friction and wear behavior under various loading conditions on test rigs or in vehicle tests. An optimized design of the system with regard to appropriate function and durability on the one hand as well as low cost, low mass and compact overall dimensions on the other hand requires extensive testing. According to the present state of knowledge, derived from numerous experimental investigations, temperature can be attributed the most significant influence on the tribology of synchronizing systems. Therefore, the influence of various loading conditions on contact temperature was investigated; a relation between temperature and tribological performance was established. The Finite Element Method was applied to simulate the thermal behavior of a synchronizing system depending on different operating conditions. A result of this simulation is the spatial and time-dependent temperature distribution in the area of contact. Characteristics of the tribological performance of a molybdenum coated

synchromesh ring in contact with a steel cone were derived from extensive experimental investigations. Significantly different friction and wear patterns can be distinguished. At heavy loading conditions the coefficient of friction is quite high and continuously severe wear occurs; light operating conditions results in a low friction coefficient, whilst no more wear is observed. Between those two extremes an indifferent regime exists, in which both patterns of tribological behavior occur.

A reason for this characteristics behavior of the system described here was found by means of the Finite Element simulation. Apparently, the friction and wear pattern depends on the temperature in the contact area; for mild wear and low friction coefficients the contact temperature must not exceed a critical value in order to avoid severe wear. Within limits the predicted tribological behavior and the test results are in good agreement. The calculation of the temperature in the contact area provides a basis for a classification of the load conditions in terms of their thermal and tribological effect, a practically applicable estimation of service life and a design procedure based on numerical simulation rather than on testing.

**J.Y.Lin et al [2]** Radial transient heat conduction in composite hollow cylinders with the temperature-dependent thermal conductivity was investigated numerically by using an application of the Laplace transform technique combined with the finite element method (FEM) or with the finite difference method (FDM). The domain of the governing equation was discretized using the FEM or FDM. The nonlinear terms were linearized by Taylor's series approximation. The time-derivatives in the linearized equations were transformed to the corresponding algebraic terms by the application of the Laplace transform. The numerical inversion of the Laplace transform was applied to invert the transformed temperatures to the temperatures in the physical quantity. Since the present method was not a time-stepping procedure, the results at a specific time can be calculated in the time domain without any step-by-step computations. To show the accuracy of the present method for the problems under consideration, a comparison of the hybrid finite element solutions with the hybrid finite difference solutions was made.

**J. Brilla et al [3]** generalized variational principles in the sense of the Laplace transform for viscoelastic problems were derived. Then mathematical theory of viscoelasticity in generalized Hardy spaces and in weighted anisotropic Sobolev spaces and spectral theory of corresponding non-self adjoint operators was elaborated. Finally the Laplace transform FEM for numerical analysis of time-dependent problems of the mathematical physics was proposed and analyzed.

**S. V. Tsinopoulos et al [4]** an advanced boundary element method was appropriately combined with the fast Fourier transform (FFT) to analyze general axisymmetric problems in frequency domain elastodynamics. The problems were characterized by axisymmetric geometry and non-axisymmetric boundary conditions. Boundary quantities were expanded in complex Fourier series in the circumferential direction and the problem was efficiently decomposed into a series of problems, which were solved by the BEM for the Fourier boundary quantities, discretizing only the surface generator of the axisymmetric body. Quadratic boundary elements were used and BEM integrations were done by FFT algorithm in the circumferential direction and by Gauss quadrature in the generator direction. Singular integrals were evaluated directly in a highly accurate way. The Fourier transformed solution was then numerically inverted by the FFT, provided the final solution. The method combines high accuracy and efficiency and this was demonstrated by illustrative numerical examples.

**H. C. Wang et al [5]** a new numerical method was proposed for the boundary element analysis of axisymmetric bodies. The method was based on complex Fourier series expansion of boundary quantities in circumferential direction, which reduces the boundary element equation to an integral equation in  $(r-z)$  plane involving the Fourier coefficients of boundary quantities, where  $r$  and  $z$  are the co-ordinates of the  $(r, \theta, z)$  cylindrical co-ordinate system. The kernels appearing in these integral equations can be computed effectively by discrete Fourier transform formulas together with the fast Fourier transform (FFT) algorithm, and the integral equations in  $(r-z)$  plane can be solved by Gaussian quadrature, which establishes the Fourier coefficients associated with boundary quantities. The Fourier transform solution can then be inverted into  $(r, \theta, z)$

space by using again discrete Fourier transform formulas together with FFT algorithm. In the study, first we presented the formulation of the proposed method which was outlined above. Then, the method was assessed by using three sample problems. A good agreement was observed in the comparisons of the predictions of the method with those available in the literature. It was further found that the proposed method provided considerable saving in computer time compared to existing methods.

**A. Floquet et al [6]** determined of temperature distribution and comparison of simulation results and experimental results in the disc by 2D thermal analysis using axisymmetric model. The disc brake used in the automobile is divided into two parts; a rotating axisymmetrical disc, and the stationary pads. The friction heat, which is generated on the interface of the disc and pads, can cause high temperature during the braking process. The influence of initial velocity and deceleration on cooling of the brake disc was also investigated. The thermal simulation is used to characterize the temperature field of the disc with appropriate boundary conditions.

A Finite-element method was developed for determining the critical sliding speed for thermo elastic instability of an axisymmetric clutch or brake. Linear perturbations on the constant-speed solution were sought that vary sinusoidally in the circumferential direction and grow exponentially in time. These factors cancel in the governing thermo elastic and heat-conduction equations, leading to a linear eigenvalue problem on the two-dimensional cross-sectional domain for the exponential growth rate for each Fourier wave number. The imaginary part of this growth rate corresponds to a migration of the perturbation in the circumferential direction. The algorithm was tested against an analytical solution for a layer sliding between two half-planes and provided excellent agreement, for both the critical speed and the migration speed. Criteria were developed to determine the mesh re-finement required to give an adequate discrete description of the thermal boundary layer adjacent to the sliding interface. The method was then used to determine the unstable mode and critical speed in geometries approximating current multi-disc clutch practice.

**R. A. Burton et al [7]** showed the thermal deformation in frictionally heated contact wheel-mounted on disc brakes were exposed to severe non-symmetrical mechanical and thermal loads. The paper described the design process for two high-performance, hub-mounted discs of different size and duty. The development was resulted in two very successful but fundamentally different hub designs and manufacturing methods. Initially, finite element analyses used in the design optimization were mainly concentrated on bulk thermal effects. Recently, in order further to improve the design process, analyses had included macro thermal effects, providing valuable results, particularly related to the prediction of disc permanent coning, one of the most critical design requirements.

Whenever friction occurs in dry sliding of mechanical components, mechanical energy is transformed into heat through surface and volumetric processes in and around the real area of contact. This frictional heating, and the thermal and thermo mechanical phenomena associated with it, can have a very important influence on the tribological behavior of the sliding components, especially at high sliding velocities. Significant developments in the study of these phenomena were reviewed. Among the topics reviewed were mechanisms of frictional heating and the distribution of heat during sliding friction, the measurement and analysis of surface and near surface temperatures resulting from frictional heating, thermal deformation around sliding contacts and the changes in contact geometry caused by thermal deformation and thermo elastic instability, and the thermo mechanical stress distribution around the frictionally heated and thermally deformed contact spots. The paper concludes with a discussion of the influence of the thermal and thermo mechanical contact phenomena on wear, thermo cracking and other modes of failure of sliding mechanical components.

**A. E. Anderson et al [8]** investigated the hot spotting in automotive friction system. When sliding occurs with significant frictional heating, thermo elastic deformation may lead to a transition from smoothly distributed asperity contact to a condition where the surfaces are supported by a few thermal asperities. This circumstance may be associated with a transition to a condition of severe wear because of the elevated contact pressure and temperature, and also because of production of tensile stresses. This second stress

component may lead to heat checking whereupon the rough checked surface acts to abrade the mating material.

**M. Comninou et al [9]** determined the stability boundary for the thermo elastic contact of a rectangular elastic block sliding against a rigid wall in the presence of a pressure-dependent thermal contact resistance. This geometry can be seen as intermediate between the idealized 'Aldo' rod model and continuum solutions for the elastic half-plane. The solution was obtained by comparing the expression for the perturbed boundary condition including frictional heating with that for purely static loading, already solved by Yeo and Barber (1995). The critical sliding speed was obtained as a function of the temperature difference imposed between the wall and the free end. In most cases, frictional heating tends to destabilize the system. However, for certain forms of the resistance-pressure law, the opposite conclusion was reached and the system can be stable for all sliding speeds. The factors influencing transition were discussed, including wear, cooling and hydrodynamic lubrication. The transition state was also discussed with regard to the stress distribution, rate of movement of the contact patches and temperatures.

**J. R. Barber et al [10,11]** developed a procedure based on the Radon transform and elements of distribution theory, to obtain fundamental thermo elastic three-dimensional (3D) solutions for thermal and/or mechanical point sources moving steadily over the surface of a half space. A concentrated heat flux was taken as the thermal source, whereas the mechanical source consists of normal and tangential concentrated loads. It is assumed that the sources move with a constant velocity along a fixed direction. The solutions obtained were exact within the bounds of Boott's coupled thermo-elastic dynamic theory, and results for surface displacements are obtained over the entire speed range (i.e. for sub-Rayleigh, super-Rayleigh/subsonic, transonic and supersonic source speeds). This problem has relevance to situations in Contact Mechanics, Tribology and Dynamic Fracture, and is especially related to the well-known heat checking problem (thermo-mechanical cracking in an unflawed half-space material from high-speed asperity excitations). Our solution technique fully exploits as auxiliary solutions the ones for the corresponding plane-strain and anti-plane shear problems by reducing the original

3D problem to two separate 2D problems. These problems were uncoupled from each other, with the first problem being thermo elastic and the second one pure elastic. In particular, the auxiliary plane-strain problem was completely analogous to the original problem, not only with regard to the field equations but also with regard to the boundary conditions. This makes the technique employed here more advantageous than other techniques, which require the prior determination of a fictitious auxiliary plane-strain problem through solving an integral equation.

**T. A. Dowat et al [12]** proposed to contribute to dynamic and thermal analysis of the braking phenomenon. A dynamic model was established. Using this model the equation of motion of a car was derived for straight line braking. In this context, firstly the pressure variations in the brake hydraulic circuit versus pedal force were determined. Afterwards, the expression for friction torques and associated braking force induced by hydraulic pressure was taken into account, and substituted into the equation of motion of vehicle. In its last form, this equation was numerically solved by means of the Newmark integration scheme; so, the distance traveled by car until stopping, along with its speed and deceleration, was computed. Finally, a thermal analysis in the brake discs and drum was carried out. An excellent agreement between numerical and test results was observed. In addition, optimal pressure values for which the rear tyre do not go to lockup was obtained.

**K.Lee et al [13, 14]** thermo elastic instability in an automotive disk brake system was investigated experimentally under drag braking conditions. The onset of instability was clearly identifiable through the observation of non uniformities in temperature measured using embedded thermocouples. A stability boundary was established in temperature/speed space, the critical temperature being attributable to temperature-dependence of the brake pad material properties. It was also found that the form of the resulting unstable perturbations or Eigen functions changes depending upon the sliding speed and temperature. A finite-element method was developed for determining the critical sliding speed for thermo elastic instability of an axis symmetric clutch or brake. Linear perturbations on the constant-speed solution were sought that vary sinusoid ally in

the circumferential direction and grow exponentially in time. These factors cancel in the governing thermo elastic and heat-conduction equations, leading to a linear Eigen value problem on the two-dimensional cross-sectional domain for the exponential growth rate for each Fourier wave number. The imaginary part of this growth rate corresponds to a migration of the perturbation in the circumferential direction. The algorithm was tested against an analytical solution for a layer sliding between two half-plane and gave excellent agreement, for both the critical speed and the migration speed. Criteria were developed to determine the mesh refinement required to give an adequate discrete description of the thermal boundary layer adjacent to the sliding interface. The method was then used to determine the unstable mode and critical speed in geometries approximating current multi-disc clutch practice.

**J. R. Barber et al [15]** the frictional heat generated during braking causes thermo elastic distortion that modifies the contact pressure distribution. If the sliding speed is sufficiently high, this can lead to frictionally-excited thermo elastic instability (TEI), characterized by major non-uniformities in pressure and temperature. In automotive applications, a particular area of concern is the relation between thermo elastically induced hot spots in the brake disks and noise and vibration in the brake system. Numerical implementation of Burrton's perturbation analysis for thermo elastic instability in a two-dimensional model provided an extremely efficient method for determining the critical speed in simple sliding systems. In this paper, the two-dimensional model has been extended to an annular three-dimensional disk model in order to consider more realistic brake and clutch geometries and to provide more accurate critical speed. The results showed that the Eigen modes exhibit focal hot spots along the circumference on each side of the disk and the thin disk is more stable than the thick disk when both disk thicknesses are below the optimal thickness.

**S. Du et al [16]** finite element method was used to reduce the problem of thermo elastic instability (TEI) for a brake disk to an Eigen value problem for the critical speed. Conditioning of the Eigen value problem was improved by performing a preliminary Fourier decomposition of the resulting matrices. Results were also obtained for two-

dimensional layer and three-dimensional strip geometries, to explore the effects of increasing geometric complexity on the critical speeds and the associated mode shapes. The hot spots were generally focal in shape for the three-dimensional models, though modes with several reversals through the width start to become dominant at small axial wave numbers  $n$ , including a thermal banding mode corresponding to  $n = 0$ . The dominant wavelength (hot spot spacing) and critical speed were not greatly affected by the three-dimensional effects, being well predicted by the two-dimensional analysis except for banding modes. Also, the most significant deviation from the two-dimensional analysis can be approximated as a monotonic interpolation between the two-dimensional critical speeds for plane stress and plane strain as the width of the sliding surface was increased. This suggested that adequate algorithms for design against TEI could be developed based on the simpler two-dimensional analysis.

**J.M.Leroy et al [17]** hard coatings were more and more used to improve the mechanical and tribological behavior of surfaces. Thermo mechanical cracking can occur in these coatings when they slide under heavy loads. A two-dimensional model of a finite thickness layered medium submitted to a moving heat source was presented. The analytical solution of the temperature and thermo elastic stress fields was obtained using Fourier transforms. The behavior of each layer was described by transfer-matrices and a relation between the displacement- and stress-vectors is given. The originality of the study was the use of a fast Fourier transform algorithm. With this method, calculation time is reduced, no singularity problems were met in the inverse transform and each parameter (especially the thickness of the layers) can be studied over a wide range

A transient analysis for thermo elastic contact problem of disk brakes with frictional heat generation was performed using the finite element method. To analyze the thermo elastic phenomenon occurring in disk brakes, the coupled heat conduction and elastic equations were solved with contact problems. The numerical simulation for the thermo elastic behavior of disk brake was obtained in the repeated brake condition. The computational results were presented for the distributions of pressure and temperature on each friction surface between the contacting bodies. Also, thermo elastic instability (TEI) phenomenon (the unstable growth of contact pressure and temperature) was investigated in this study, and the influence of the material properties on the thermo elastic behaviors

(the maximum temperature and contact ratio on the friction surfaces) was investigated to facilitate the conceptual design of the disk brake system. Based on these numerical results, the thermo elastic behaviors of the carbon–carbon composites with excellent mechanical and thermal properties were also discussed.

**H. W. Gonaska et al [18]** four automotive friction system hot spot types were introduced and discussed. These were asperity, focal, distortional, and regional. Friction material and metal counter surface wear consequences were discussed, as they related to the different hot spotting types. Focal hot spots were emphasized. These may form martensite on the cast iron drum or disk rubbing surface. Such hot spots, if not prevented, can provide a root cause for unacceptable performance or durability in automotive friction systems. Computer studies, using a two-dimensional model, were used to complement the experimental studies of critical hot spots and determine hot spot thermal flux limits. Surface melting and known requirements for the formation of martensite were used to establish bounds from the computer analysis.

**J. E. Akin et al [19]** studied the geometry of two flat plates contacting on a straight common edge with sliding parallel to the line of contact, conditions were found where pressure perturbations on the interface will grow, diminish or remain unchanged. The effects of materials properties, friction coefficient, and sliding speed were delineated. Conditions which lead to a growing disturbance may be thought of as undesirable in that they lead to locally increased contact loading as well as locally increased temperatures. Adjacent to the regions of increased pressure are regions of reduced pressure where the surfaces may part, and give rise to leakage when the line of contact is considered to represent the lip of a seal. It was shown that materials sliding on their own kind tend to be stable relative to this phenomenon, while good thermal conductors sliding on good thermal insulators must always have some characteristic sliding speed above which instability will occur.

The objective of this research is to advance a technique for simulating a three dimensional disk brake system, clutches, and mechanical seals. Due to its tremendous

time and cost requirements, there are no known works on instability simulation evolving via a stable region, but excellent efforts on determining instability conditions using eigenvalue formulation have been reported by Barber and coworkers [10, 11]. For the purpose of design and analysis, understanding of the both transient behaviors and post-instability is of paramount importance in the industry. Thus, in this study we introduce a potential computation technique.

In this study we discretize the domain using finite elements, enables us to reach a very efficient computation technique that has the ability to invoke a fast transient thermo elastic solution and thermo elastic instability as well. This study proposed the aforementioned technique to shed some light on a possibly fast and practically applicable numerical analysis in the field of frictionally induced thermo mechanical coupled problems, such as a disk brake system, clutches, and mechanical seals. By applying the proposed technique, we solved some temperature and displacement fields for a three – dimensional brake system. However, we did not discuss in a quantitative sense the computation results through comparison with experiments for validation since we have not found appropriate technique to solid-type disk instead of ventilated-type disks, for which experimental data can be found in [13,14]. Authors currently are investigating the application of this technique to a ventilated-type disk problem.

# **CHAPTER - 3**

## **FINITE ELEMENT ANALYSIS**

### **3.1 INTRODUCTION**

The finite element method is numerical analysis technique for obtaining approximate solutions to a wide variety of engineering problems. Because of its diversity and flexibility as an analysis tool, it is receiving much attention in almost every industry. In more and more engineering situations today, we find that it is necessary to obtain approximate solutions to problem rather than exact closed form solution.

It is not possible to obtain analytical mathematical solutions for many engineering problems. An analytical solutions is a mathematical expression that gives the values of the desired unknown quantity at any location in the body, as consequence it is valid for infinite number of location in the body. For problems involving complex material properties and boundary conditions, the engineer resorts to numerical methods that provide approximate, but acceptable solutions.

The finite element method has become a powerful tool for the numerical solutions of a wide range of engineering problems. It has been developed simultaneously with the increasing use of the high- speed electronic digital computers and with the growing emphasis on numerical methods for engineering analysis. This method started as a generalization of the structural idea to some problems of elastic continuum problem, started in terms of different equations.

### **3.2 PROCEDURE FOR ANSYS ANALYSIS**

Static analysis is used to determine the displacements stresses, strains and forces in structures or components due to loads that do not induce significant inertia and damping effects. Steady loading in response conditions are assumed. The kinds of loading that can be applied in a static analysis include externally applied forces and pressures, steady

state inertial forces such as gravity or rotational velocity imposed (non-zero) displacements, temperatures (for thermal strain).

A static analysis can be either linear or non linear. In our present work we consider linear static analysis.

The procedure for static analysis consists of these main steps

- Building the model
- Obtaining the solution
- Reviewing the results.

### **3.2.1 BUILD THE MODEL**

In this step we specify the job name and analysis title use PREP7 to define the element types, element real constants, material properties and model geometry element type both linear and non- linear structural elements are allowed. The ANSYS elements library contains over 80 different element types. A unique number and prefix identify each element type.

E.g. BEAM 94, PLANE 71, SOLID 96 and PIPE 16

### **3.2.2 MATERIAL PROPERTIES**

Young's modulus (EX) must be defined for a static analysis. If we plan to apply inertia loads (such as gravity) we define mass properties such as density (DENS). Similarly if we plan to apply thermal loads (temperatures) we define coefficient of thermal expansion (ALPX).

### **3.2.3 SOLUTION**

In this step we define the analysis type and options, apply loads and initiate the finite element solution. This involves three phases:

- Pre-processor phase
- Solution phase
- Post-processor phase

**Pre-processor:**

Pre processor has been developed so that the same program is available on micro, mini, super-mini and mainframe computer system. This allows easy transfer of models one system to other.

The following Table 3.1 shows the brief description of steps followed in each phase:

Table No. – 3.1

<b>PREPROCESSOR PHASE</b>	<b>SOLUTION PHASE</b>	<b>POST-PROCESSOR PHASE</b>
<b>GEOMETRY DEFINITIONS</b>	<b>ELEMENT MATRIX FORMULATION</b>	<b>POST SOLUTION OPERATIONS</b>
<b>MESH GENERATION</b>	<b>OVERALL MATRIX TRIANGULARIZATION</b>	<b>POST DATA PRINT OUT (FOR REPORTS)</b>
<b>MATERIAL DEFINITIONS</b>	<b>(WAVE FRONT)</b>	<b>POST DATA</b>
<b>CONSTRAINT DEFINITIONS</b>	<b>DISPLACEMENT, STRESS, ETC.</b>	<b>SCANNING POST DATA DISPLAY</b>
<b>LOAD DEFINITION</b>	<b>CALCULATION</b>	
<b>MODEL DISPLAY</b>		

Pre processor is an interactive model builder to prepare the FE (finite element) model and input data. The solution phase utilizes the input data developed by the pre processor, and prepares the solution according to the problem definition. It creates input files to the temperature etc. on the screen in the form of contours.

**Geometrical definitions:**

There are four different geometric entities in pre processor namely key points, lines, area and volumes. These entities can be used to obtain the geometric representation of the structure. All the entities are independent of other and have unique identification labels.

**Model Generations:**

Two different methods are used to generate a model:

- Direct generation.
- Solid modeling

With solid modeling we can describe the geometric boundaries of the model, establish controls over the size and desired shape of the elements and then instruct ANSYS program to generate all the nodes and elements automatically. By contrast, with the direct generation method, we determine the location of every node and size shape and connectivity of every element prior to defining these entities in the ANSYS model. Although, some automatic data generation is possible (by using commands such as FILL, NGEN, EGEN etc) the direct generation method essentially a hands on numerical method that requires us to keep track of all the node numbers as we develop the finite element mesh. This detailed book keeping can become difficult for large models, giving scope for modeling errors. Solid modeling is usually more powerful and versatile than direct generation and is commonly preferred method of generating a model.

**Mesh generation:**

In the finite element analysis the basic concept is to analyze the structure, which is an assemblage of discrete pieces called elements, which are connected, together at a finite number of points called Nodes. Loading boundary conditions are then applied to these elements and nodes. A network of these elements is known as Mesh.

**Finite element generation:**

The maximum amount of time in a finite element analysis is spent on generating elements and nodal data. Pre processor allows the user to generate nodes and elements automatically at the same time allowing control over size and number of elements. There are various types of elements that can be mapped or generated on various geometric entities.

The elements developed by various automatic element generation capabilities of pre processor can be checked element characteristics that may need to be verified before the finite element analysis for connectivity, distortion-index etc.

Generally, automatic mesh generating capabilities of pre processor are used rather than defining the nodes individually. If required nodes can be defined easily by defining the allocations or by translating the existing nodes. Also one can plot, delete, or search nodes.

**Boundary conditions and loading:**

After completion of the finite element model it has to constrain and load has to be applied to the model. User can define constraints and loads in various ways. All constraints and loads are assigned set ID. This helps the user to keep track of load cases.

**Model display:**

During the construction and verification stages of the model it may be necessary to view it from different angles. It is useful to rotate the model with respect to the global system and view it from different angles. Pre processor offers this capabilities. By windowing feature pre processor allows the user to enlarge a specific area of the model for clarity and details. Pre processor also provides features like smoothness, scaling, regions, active set, etc for efficient model viewing and editing.

**Material defections:**

All elements are defined by nodes, which have only their location defined. In the case of plate and shell elements there is no indication of thickness. This thickness can be given

as element property. Property tables for a particular property set 1-D have to be input. Different types of elements have different properties for e.g.

Beams: Cross sectional area, moment of inertia etc

Shell: Thickness

Springs: Stiffness

Solids: None

The user also needs to define material properties of the elements. For linear static analysis, modulus of elasticity and Poisson's ratio need to be provided. For heat transfer, coefficient of thermal expansion, densities etc. are required. They can be given to the elements by the material property set to 1-D.

### **Solution:**

The solution phase deals with the solution of the problem according to the problem definitions. All the tedious work of formulating and assembling of matrices are done by the computer and finally displacements and stress values are given as output. Some of the capabilities of the ANSYS are linear static analysis, non linear static analysis, transient dynamic analysis, etc.

### **Post- processor:**

It is a powerful user- friendly post- processing program using interactive colour graphics. It has extensive plotting features for displaying the results obtained from the finite element analysis. One picture of the analysis results (i.e. the results in a visual form) can often reveal in seconds what would take an engineer hour to assess from a numerical output, say in tabular form. The engineer may also see the important aspects of the results that could be easily missed in a stack of numerical data.

Employing state of art image enhancement techniques, facilities viewing of:

- Contours of stresses, displacements, temperatures, etc.
- Deform geometric plots
- Animated deformed shapes

- Time-history plots
- Solid sectioning
- Hidden line plot
- Light source shaded plot
- Boundary line plot etc.

The entire range of post processing options of different types of analysis can be accessed through the command/menu mode there by giving the user added flexibility and convenience.

### 3.3 FINITE ELEMENT FORMULATION FOR HEAT CONDUCTION

The unsteady heat conduction equation of each body for an axis-Symmetric problem described in the cylindrical coordinate system is given as follows:

$$\rho c \frac{\partial T}{\partial t} = \frac{1}{r} \frac{\partial}{\partial r} \left( r k_r \frac{\partial T}{\partial r} \right) + \frac{\partial}{\partial z} \left( k_z \frac{\partial T}{\partial z} \right) \quad (3.1)$$

With the boundary conditions and initial condition

$$T = T^* \quad \text{on } \Gamma_0 \quad (3.2)$$

$$q_n = h (T - T_\infty) \quad \text{on } \Gamma_1 \quad (3.3)$$

$$q_n = q_n^* \quad \text{on } \Gamma_2 \quad (3.4)$$

$$T = T_0 \quad \text{at } t = 0 \quad (3.5)$$

Where  $\rho$ ,  $c$ ,  $k_r$  and  $k_z$  are the density, specific heat and thermal conductivities in r and z direction of the material, respectively. Also,  $T^*$  is the prescribed temperature, h the heat transfer coefficient,  $q_n^*$  the heat flux at each contact interface due to friction,  $T_\infty$  the ambient temperature,  $T_0$  the initial temperature and  $\Gamma_0$ ,  $\Gamma_1$  and  $\Gamma_2$  are the boundaries on which temperature, convection and heat flux are imposed, respectively.

Using Galerkin's approach, a finite element formulation of unsteady heat Eq. (3.1) can be written in the following matrix form as

$$C_T \dot{T} + KH_T T = R \quad (3.6)$$

Where  $C_T$  is the capacity matrix,  $KH_T$  is the conductivity matrix. T and R and are the nodal temperature and heat source vector, respectively.

The most commonly used method for solving Eq. (3.6) is the direct integration method based on the assumption that temperature  $T_t$  at time t and temperature  $T_{t+\Delta t}$  at time  $t+\Delta t$  have the following relation:

$$T_{t+\Delta t} = T_t + \left[ (1 - \beta) \dot{T} + \beta \dot{T}_{t+\Delta t} \right] \Delta t \quad (3.7)$$

Eq.(3.7) can be used to reduce the ordinary differential Eq.(3.6) to the following implicit algebraic equation:

$$(C_T + b_1 KH_T) T_{t+\Delta t} = (C_T - b_2 KH_T) T_t + b_2 R_t + b_1 R_{t+\Delta t} \quad (3.8)$$

Where the variable  $b_1$  and  $b_2$  are given by

$$b_1 = \beta \Delta t, \quad b_2 = (1 - \beta) \Delta t \quad (3.9)$$

For different values of  $\beta$ , the well-known numerical integration scheme can be obtained [23].in this study,  $0.5 \leq \beta \leq 1.0$  was used, which is an unconditionally stable scheme.

### 3.4 FINITE ELEMENT FORMULATION FOR ELASTIC PROBLEM

The constitutive equation for the elastic problem with thermal expansion can be written as:

$$\sigma = D (\varepsilon - \varepsilon_0) \quad (3.10)$$

Where  $\sigma$  and  $\varepsilon_0 (\alpha \Delta t)$  are the stress and initial strain vector, respectively, and D and  $\alpha$  are the elasticity matrix and thermal expansion coefficient vector, respectively.

In order to derive the equation of equilibrium for thermo elastic problems, the variational principle was applied [24], resulting in thermo elastic finite element equation of equilibrium in the following form:

$$K U = P_f + P_t + P_{\Delta T} \quad (3.11)$$

Where K is the stiffness matrix, U the vector of nodal displacements,  $P_f$ ,  $P_t$  and  $P_{\Delta T}$  are the body force, surface traction and thermal load vector, respectively.

### 3.5 CONTACT MODEL OF DISK BRAKE

In the numerical modeling of contact problems, special attention is required because the actual contact area between the contacting bodies is usually not known beforehand. In contact problem, unlike other boundary problems, nodes on the contact surface do not have prescribed displacements or traction. Instead, they must satisfy two relationships:

1. The continuity of normal displacements on the contact surface (no overlap condition of contact area),
2. The equilibrium condition (equal and opposite traction).

Even if the contacting bodies are linear material, contact problems are nonlinear because the contact area does not change linearly with the applied load. Accordingly, iterative or increment scheme is needed to obtain the accurate solutions of contact problems. The iteration to obtain the actual contact surface are finished when all these conditions are met [25].

Fig 3.1 shows the interfaces of two adjacent sub regions i and j of the elastic bodies. The elastic contact problem is treated as quasi-static with standard unilateral contact conditions at the interface. The following constraint conditions of displacements are imposed on each interface:

$$\omega_i = \omega_j, \quad \text{if } P > 0 \quad (3.12)$$

$$\omega_i \leq \omega_j, \quad \text{if } P = 0 \quad (3.13)$$

Where  $P$  is the normal pressure on the friction surface.

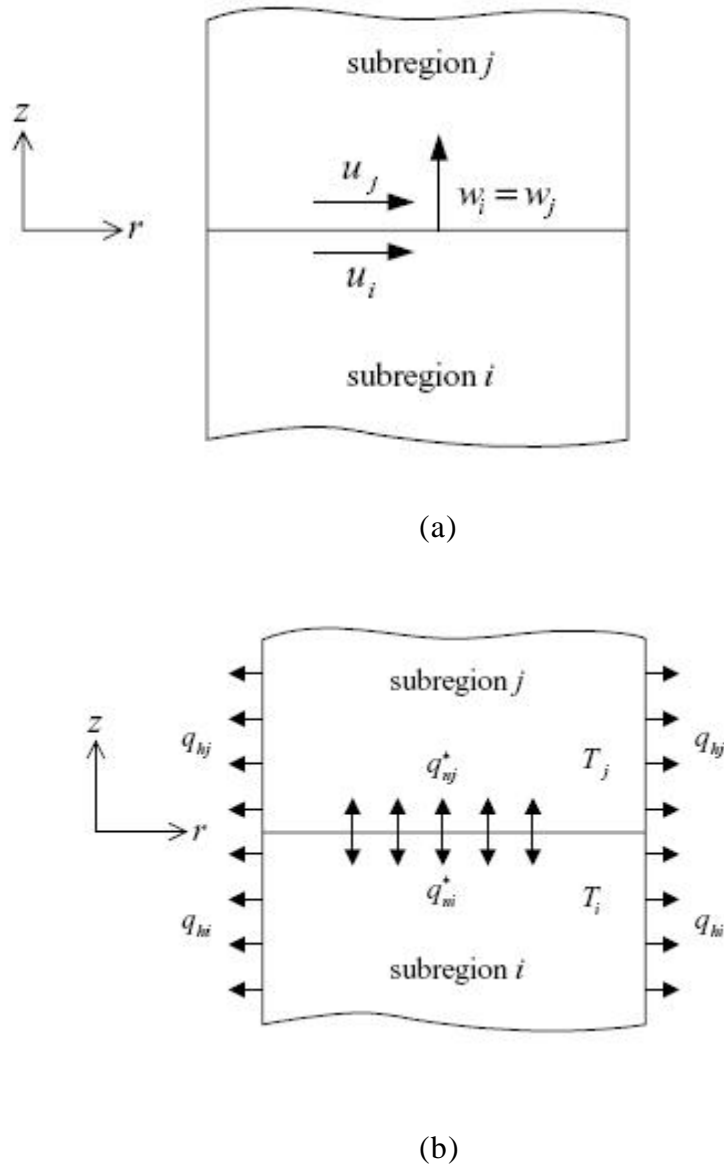


Fig. 3.1 Contact model for the (a) elastic and (b) heat conduction problem in two adjacent sub region.

The radial component of the sliding velocity resulting from the deformation is considerably smaller than the circumferential component. Therefore, the frictional forces in radial direction on the friction surface are disregarded in this study [19]. Fig 3.1(b) shows thermal phenomena of two adjacent sub regions of bodies. The interfacial thermal boundary conditions

depend on the state of mechanical contact. Two unknown terms  $q_{ni}^*$  and  $q_{nj}^*$  exist on each interface. To fully define the heat transfer problem, two additional conditions are required on each contact interface. If the surfaces are in contact, the temperature continuity condition and the heat balance condition are imposed on each interface:

$$T_i = T_j, \quad \text{if } P > 0 \quad (3.14)$$

$$q^* = \mu r \omega P = - \sum q_n^* = - (q_{ni}^* + q_{nj}^*), \quad \text{if } P > 0 \quad (3.15)$$

Where  $\mu$  and  $\omega$  are the coefficient of friction and angular sliding velocity, respectively. Then, using the aforementioned conditions, equations of one node from each pair of contact nodes are removed. If the surfaces are not in contact, the separated surfaces are treated as adiabatic conditions:

$$q^* = 0 = (q_{ni}^* = q_{nj}^*), \quad \text{if } P = 0 \quad (3.16)$$

The distribution of normal pressure  $P$  in Eq. (3.15) can be obtained by solving the mechanical problem occurring in disk.

### 3.6 FINITE ELEMENTS MODEL OF DISK BRAKE

Fig 3.2 shows the elastic finite element model of disk brakes with boundary conditions. The inner radius, outer radius, and thickness of a disk are as 0.08, 0.131 and 0.024m, respectively. The thickness of pad is 0.010m. The hydraulic pressure is applied to the boundary along radius of the piston side pad and the immobility condition in the axial direction is applied to the boundary along the radius of the finger side one. The heat finite element model of disk brakes with boundary conditions are shown in Fig 3.3. The convective boundary conditions are imposed on all boundaries to consider more realistic heat conditions. The initial temperature is  $T_0 = 20^\circ C$  in this study.

In the thermo elastic analysis of disk brakes, the most important variables are the pressure and temperature on the friction surface. To efficiently obtain accurate solution of this problem, an appropriate finite element division is

indispensable. In this study axis-symmetry 20 node 90 elements were used for the finite element analysis.

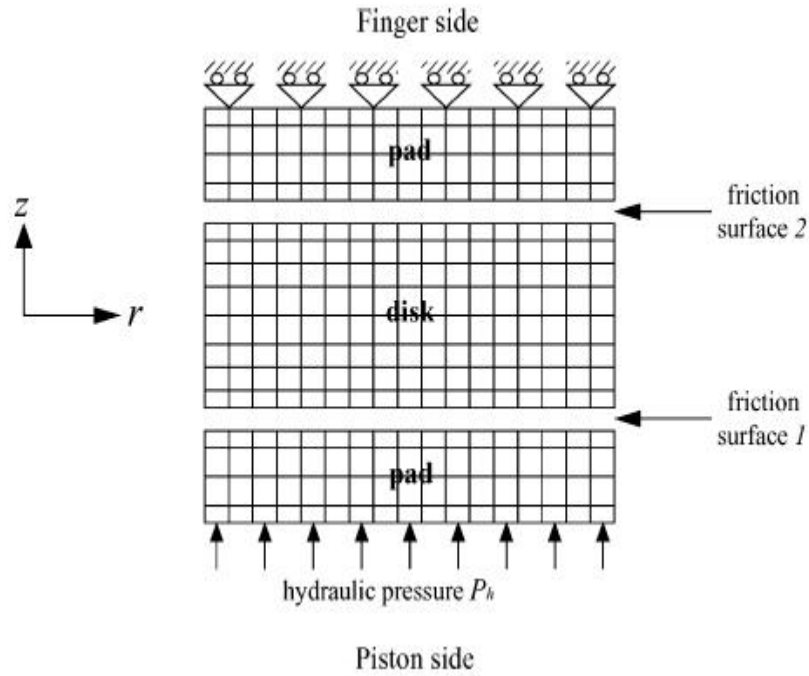


Fig 3.2 Elastic finite element model for the transient thermo elastic analysis.

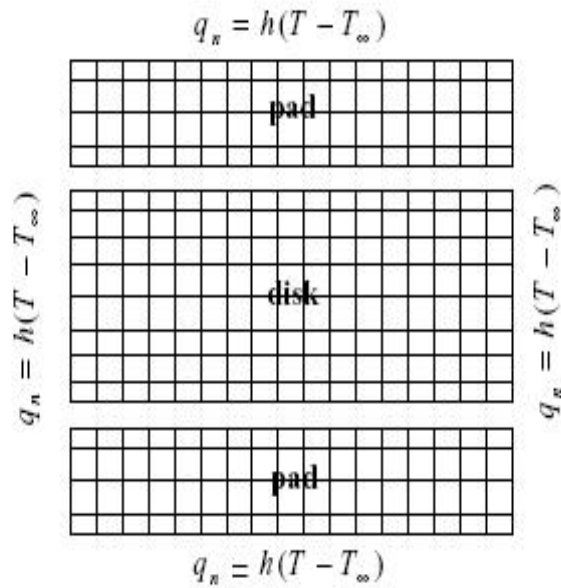


Fig 3.3. Elastic finite element model for the transient thermo elastic analysis.

### 3.7 TRANSIENT THERMO ELASTIC ANALYSIS

The present study is based on the coupled theory in which temperatures and displacements are mutually influenced. If the solution is known at time  $t$ , the solution for next time step  $t + \Delta t$  needs the information of  $R_{t+\Delta t}$  on the right hand side of Eq. (3.8). However, the distributions of pressure  $P$  on the friction surfaces at this time step, which appear in the thermal boundary conditions of Eq. (3.15), are unknown. When solving the frictional contact problems in time domain, Zagrodzki [19] assumed the contact pressure  $P$  to be the change in time of the total force represented by the applied hydraulic pressure  $P_h$  of the known time function as follows:

$$P(t + \beta \Delta t, r) \approx P(t, r) \frac{P_h(t + \beta \Delta t)}{P_h(t)} \quad (3.17)$$

However, the solution using the assumption of Eq.(3.17) are generally unreasonable in case of the variation in time of contact area or specially, the drag braking condition(constant hydraulic pressure  $P_h$  ).consequently, for the frictional contact problems where the time evolution of contact pressure is important, the fully implicit scheme should be used.

The numerical simulation for the coupled transient thermo elastic contact problem is carried out in the following way: At time  $t$ , it is assumed that the temperature distribution is  $T$  is given. Using this temperature, the thermal load vector  $P_{\Delta T}$  in Eq. (3.11) can be obtained. To solve the contact problem, elastic Eq. (3.11) is iteratively calculated to satisfy the no overlap condition and the equilibrium state on the contact surface. As a result of this calculation, new pressure distribution and new contact conditions on the contact surfaces can be obtained. Then, using new heat flux vector  $R$  in Eq. (3.8) constructed from relation of Eq. (3.15) and new contact conditions, the heat Eq. (3.8) and elastic Eq. (3.11) can be solved at time  $t + \Delta t$  . The fully implicit transient iteration are

repeated to calculate the equilibrium state of the coupled thermo elastic equations at every time step. In this way, the solution of thermo elastic state at any time could be obtained.

### **3.7.1 THERMAL ANALYSIS**

A thermal analysis calculates the temperature distribution and related thermal quantities in brake disk. Typical thermal quantities are:

1. The temperature distribution
2. The amount of heat lost or gained
3. Thermal fluxes

#### **Types of thermal analysis:**

1. A steady state thermal analysis determines the temperature distribution and other thermal quantities under steady state loading conditions. A steady state loading condition is a situation where heat storage effects varying over a period of time can be ignored.
2. A transient thermal analysis determines the temperature distribution and other thermal quantities under conditions that varying over a period of time.

#### **Planning the analysis:**

In this step a compromise between the computer time and accuracy of the analysis is made. The various parameters set in analysis are given below:

##### Thermal modeling

- Analysis type – thermal h-method.
- Steady state or Transient? Transient
- Thermal or Structural? Thermal
- Properties of the material? Isotropic
- Objective of analysis- to find out the temperature distribution in the brake disk when the process of braking is done.
- Units- SI

### **3.7.2 STRUCTURAL ANALYSIS**

Structural analysis is the most common application of the finite element analysis. The term structural implies civil engineering structure such as bridge and building, but also naval, aeronautical and mechanical structure such as ship hulls, aircraft bodies and machine housing as well as mechanical components such as piston, machine parts and tools.

#### **Types of structural analysis:**

The seven types of structural analyses in ANSYS. One can perform the following types of structural analysis. Each of these analysis types are discussed as follows:

- Static analysis
- Modal analysis
- Harmonic analysis
- Transient dynamic analysis
- Spectrum analysis
- Buckling analysis
- Explicit dynamic analysis

#### **Structural static analysis:**

A static analysis calculates the effects of steady loading conditions on a structure, while ignoring inertia and damping effects such as those caused by time varying loads. A static analysis can, however include steady inertia loads (such as gravity and rotational velocity), and time varying loads that can be approximated as static equivalent loads (such as static equivalent wind and seismic loads).

# CHAPTER - 4

## MODELING AND ANALYSIS

It is very difficult to exactly model the brake disk, in which there are still researches are going on to find out transient thermo elastic behavior of disk brake during braking applications. There is always a need of some assumptions to model any complex geometry. These assumptions are made, keeping in mind the difficulties involved in the theoretical calculation and the importance of the parameters that are taken and those which are ignored. In modeling we always ignore the things that are of less importance and have little impact on the analysis. The assumptions are always made depending upon the details and accuracy required in modeling.

The assumptions which are made while modeling the process are given below:-

1. The disk material is considered as homogeneous and isotropic.
2. The domain is considered as axis-symmetric.
3. Inertia and body force effects are negligible during the analysis.
4. The disk is stress free before the application of brake.
5. Brakes are applied on the entire four wheels.
6. The analysis is based on pure thermal loading and vibration and thus only stress level due to the above said is done. The analysis does not determine the life of the disk brake.
7. Only ambient air-cooling is taken into account and no forced Convection is taken.
8. The kinetic energy of the vehicle is lost through the brake disks i.e. no heat loss between the tyre and the road surface and deceleration is uniform.
9. The disk brake model used is of solid type and not ventilated one.
10. The thermal conductivity of the material used for the analysis is uniform throughout.

11. The specific heat of the material used is constant throughout and does not change with temperature.

#### 4.1 DEFINITION OF PROBLEM DOMAIN

Due to the application of brakes on the car disk brake rotor, heat generation takes place due to friction and this thermal flux has to be conducted and dispersed across the disk rotor cross section. The condition of braking is very much severe and thus the thermal analysis has to be carried out. The thermal loading as well as structure is axis-symmetric. Hence axis-symmetric analysis can be performed, but in this study we performed 3-D analysis, which is an exact representation for this thermal analysis. Thermal analysis is carried out and with the above load structural analysis is also performed for analyzing the stability of the structure.

#### 4.2 DIMENSIONS OF DISK BRAKE

The dimensions of brake disk used for transient thermal and static structural analysis are shown in Fig. 4.1 and Fig 4.2..

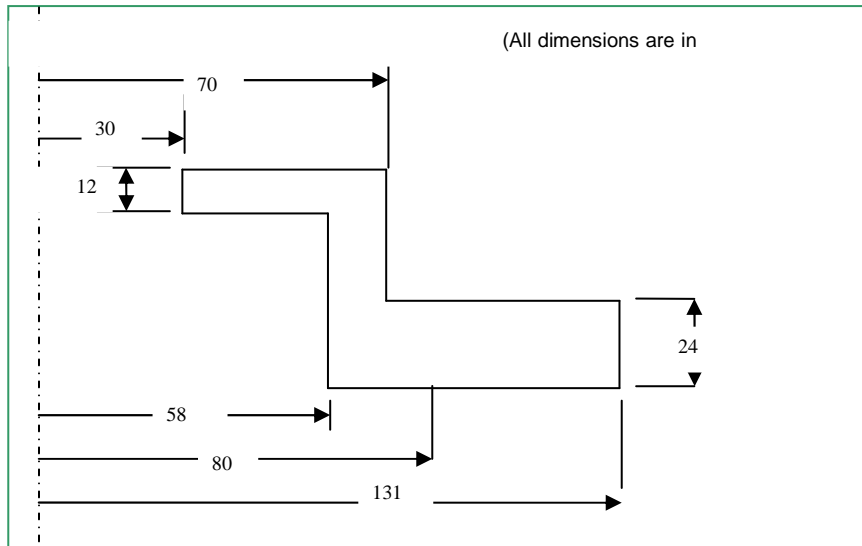


Fig. 4.1 Dimension of 24mm Disk brake

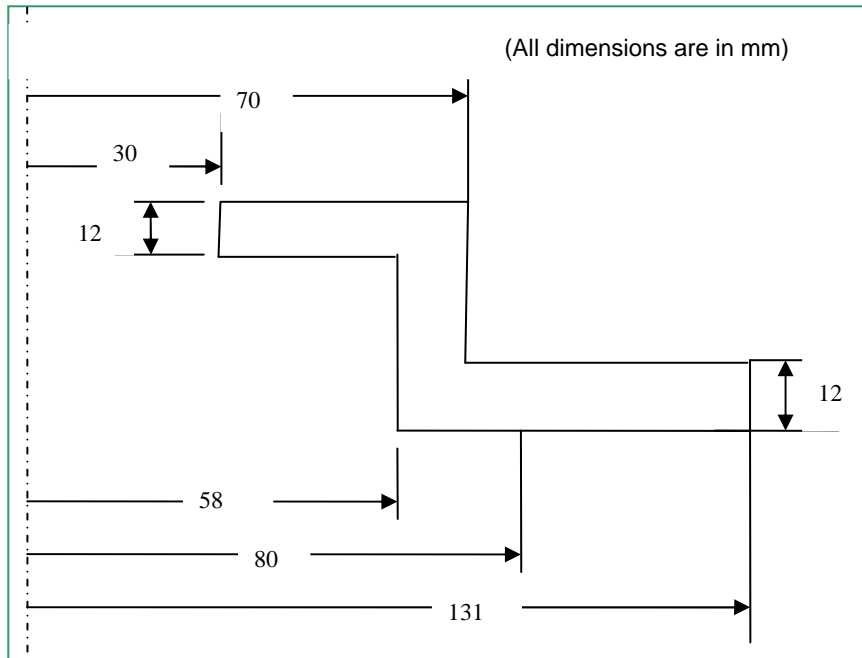


Fig. 4.2 Dimension of 12 mm Disk

### 4.3 CREATING A FINITE ELEMENT MESH

According to given specifications the element type chosen is solid 90. Solid 90 is higher order version of the 3-D eight node thermal element (Solid 70). The element has 20 nodes with single degree of freedom, temperature, at each node. The 20-node elements have compatible temperature shape and are well suited to model curved boundaries.

The 20-node thermal element is applicable to a 3-D, steady state or transient thermal analysis. If the model containing this element is also to be analyzed structurally, the element should be replaced by the equivalent structural element (Solid 95).

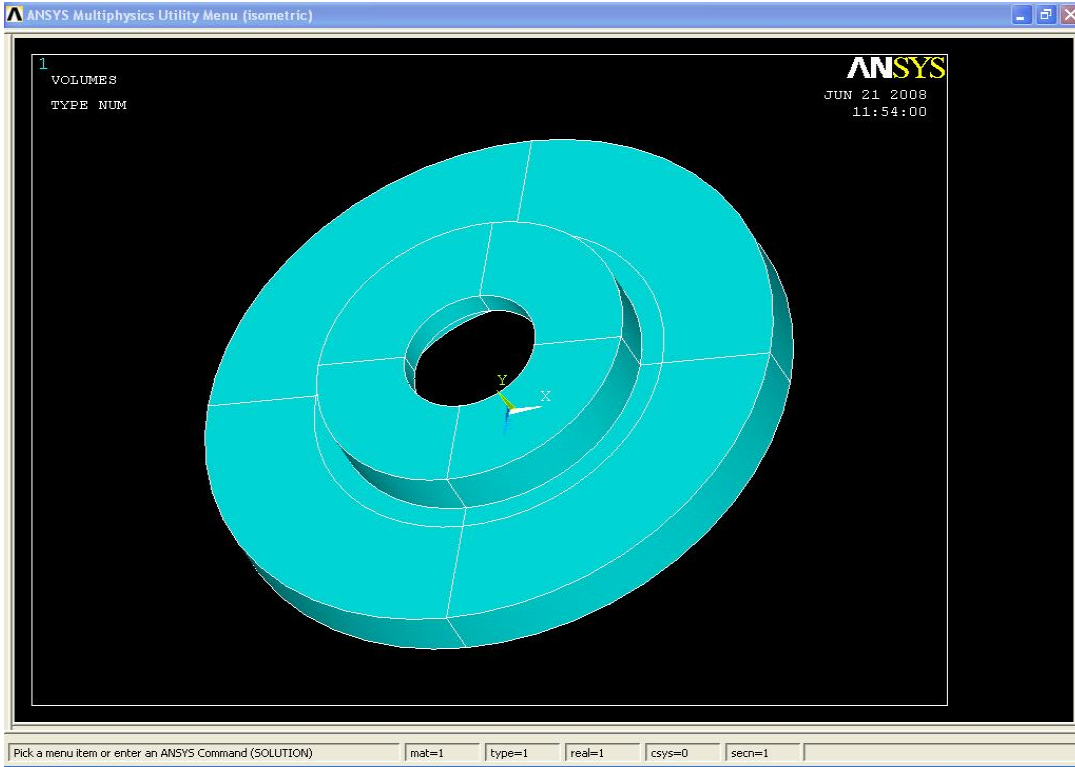


Fig. 4.3 Model of 24mm Disk brake

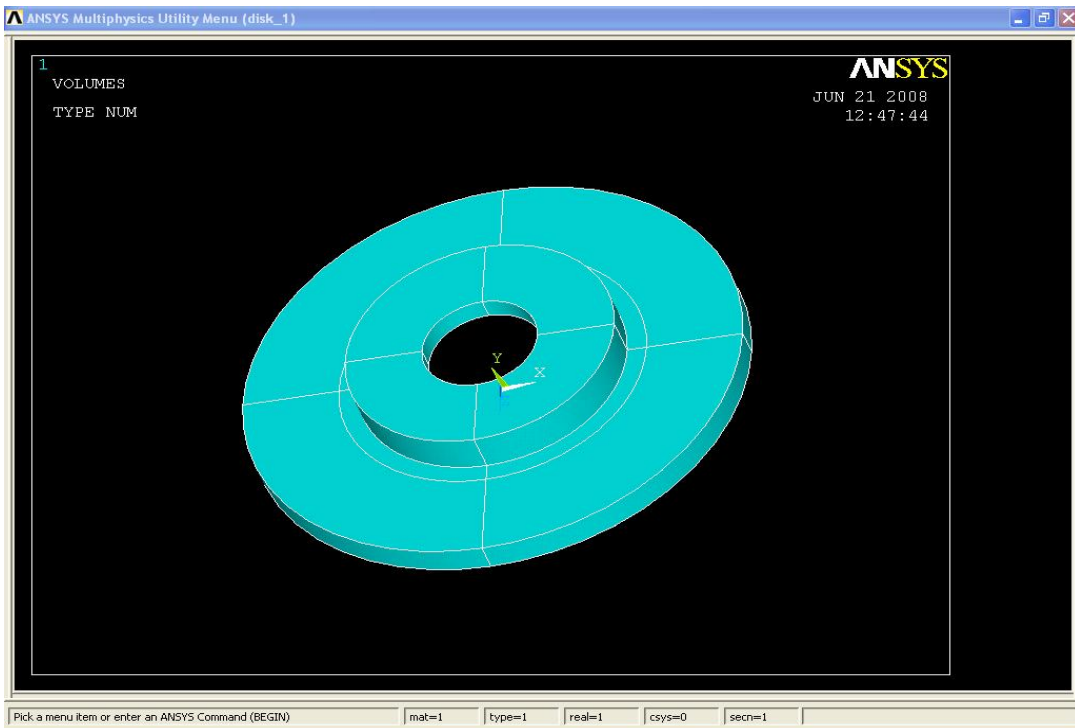


Fig. 4.4 Model of 16mm Disk brake

## 4.6 SOLID90 ELEMENT GEOMETRY

The geometry, node locations, and the coordinate system for this element are shown in Fig. 4.5. The element is defined by 20-node points and the material properties. A prism-shaped element may be formed by defining duplicate K, L, and S; A and B, and O, P, and W node numbers. A tetrahedral-shaped element and a pyramid-shaped element may also be formed as shown in Fig. 4.5.

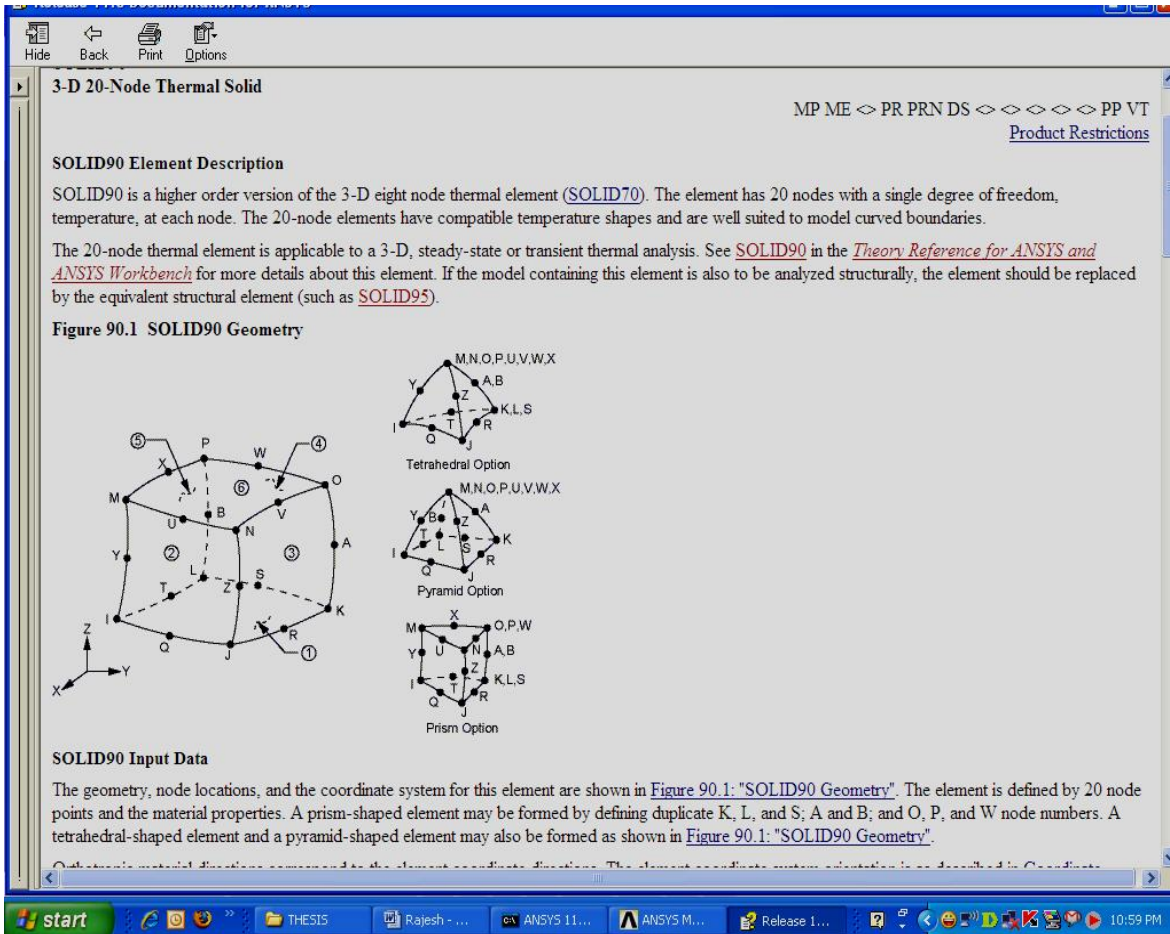


Fig 4.5 Solid element geometry

Element loads are described in node and element loads. Convection or heat flux (but not both) and radiation may be input as surface loads at the element faces as shown by the circled numbers on Fig. 4.5. Heat generation rates may be input as element body loads at the nodes. If the node I heat generation rate HG (I) is input, and all others are

unspecified, they default to HG (I). If all corner node heat generation rates are specified, each mid side node heat generation rate defaults to the average heat generation rate of its adjacent corner nodes.

### SOLID90 Input Summary

- |                        |  |
|------------------------|--|
| 1. Nodes               | I, J, K, L, M, N, O, P, Q, R, S, T, U, V, W, X, Y, Z, A, B |
| 2. Degrees of Freedom  | Temperature  |
| 3. Real Constants      | None   |
| 4. Material Properties | KXX, KYY, KZZ, DENS, C, ENTH                               |
| 5. Surface Loads       | Convection or Heat Flux (but not both) and Radiation.      |

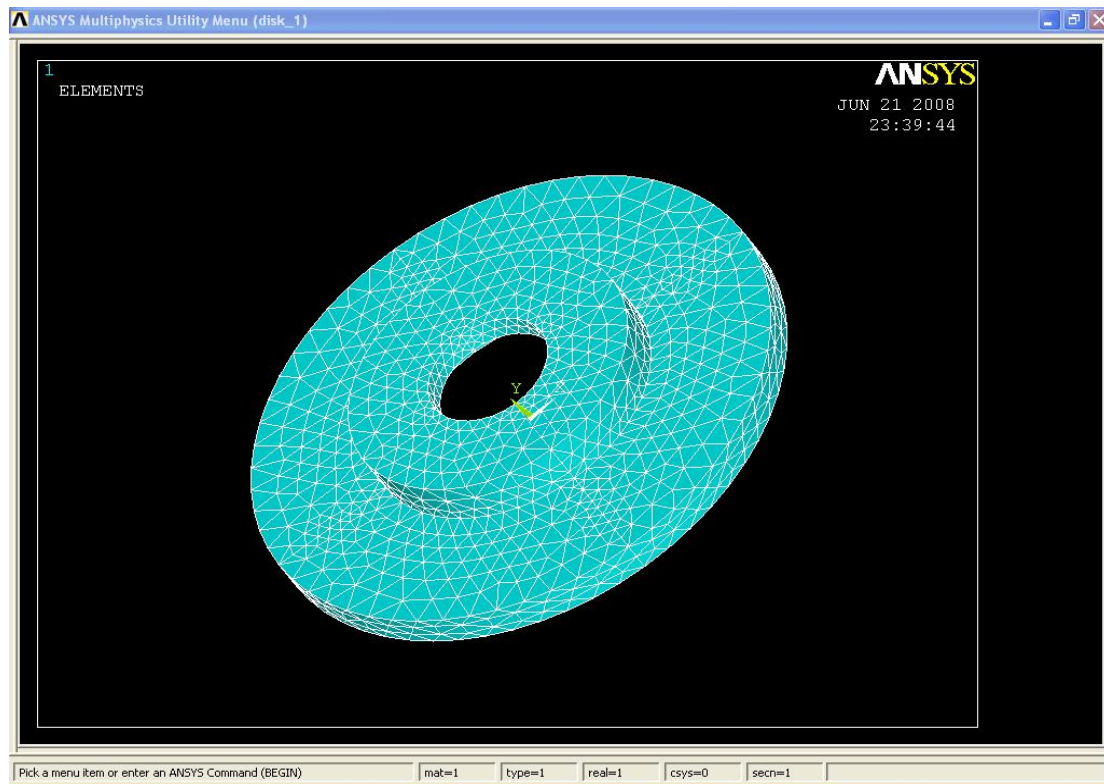


Fig. 4.6 3-D Meshed Model

## 4.7 APPLYING THE BOUNDARY CONDITIONS

In thermal and structural analysis of disk brake, we have to apply thermal and boundary conditions on 3-D disk model of disk brake.

### 4.7.1 THERMAL BOUNDARY CONDITIONS

As shown in Fig. 4.7 a model presents a three dimensional solid disk squeezed by two finite-width friction material called pads. The entire surface,  $S$ , of the disk has three different regions including  $S_1$  and  $S_2$ . On  $S_1$  heat flux is specified due to the frictional heating between the pads and disk, and  $S_2$  is defined for the convection boundary. The rest of the region, except  $S_1 \cup S_2$ , is either temperature specified or assumed to be insulated: the inner and outer rim area of disk.

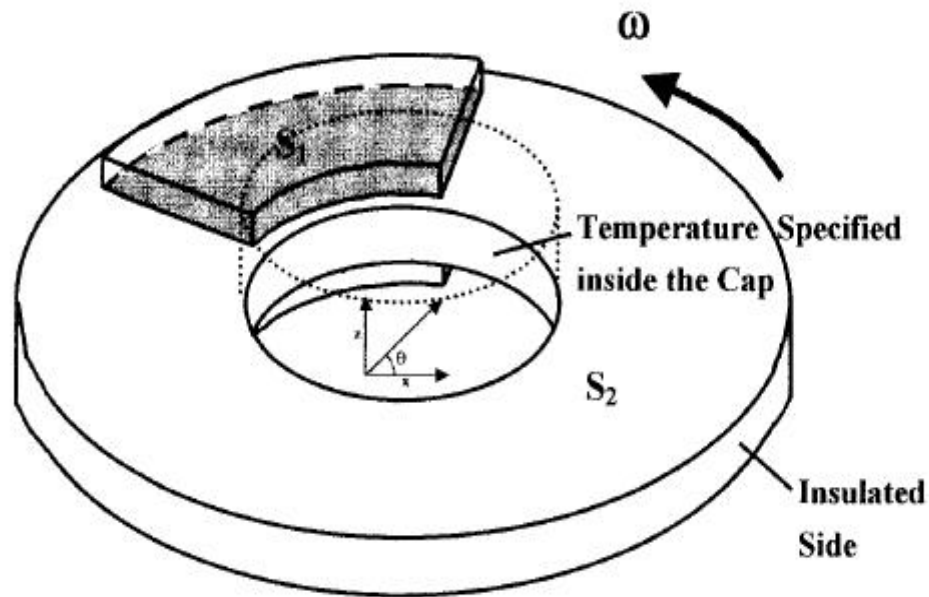


Fig. 4.7 Thermal model of Disk brake

In the contact region  $S_1$ , the local shear traction cause frictional heating that flows into the disk and pads. Heat flux  $q$  on a contact area is updated per the pressure distribution at every simulation step

$$q = \mu V P = \mu \omega r P \quad (4.1)$$

Where  $\mu$  is the coefficient of friction,  $V$  the sliding speed,  $P$  the contact pressure, and  $\omega$  is used for angular velocity.

## 4.7.2 STRUCTURAL BOUNDARY CONDITIONS

Since the axis-symmetric model is considered all the nodes on the hub radius are fixed. So the nodal displacements in the hub become zero i.e. in radial, axial and angular directions, as shown in Fig 4.8.

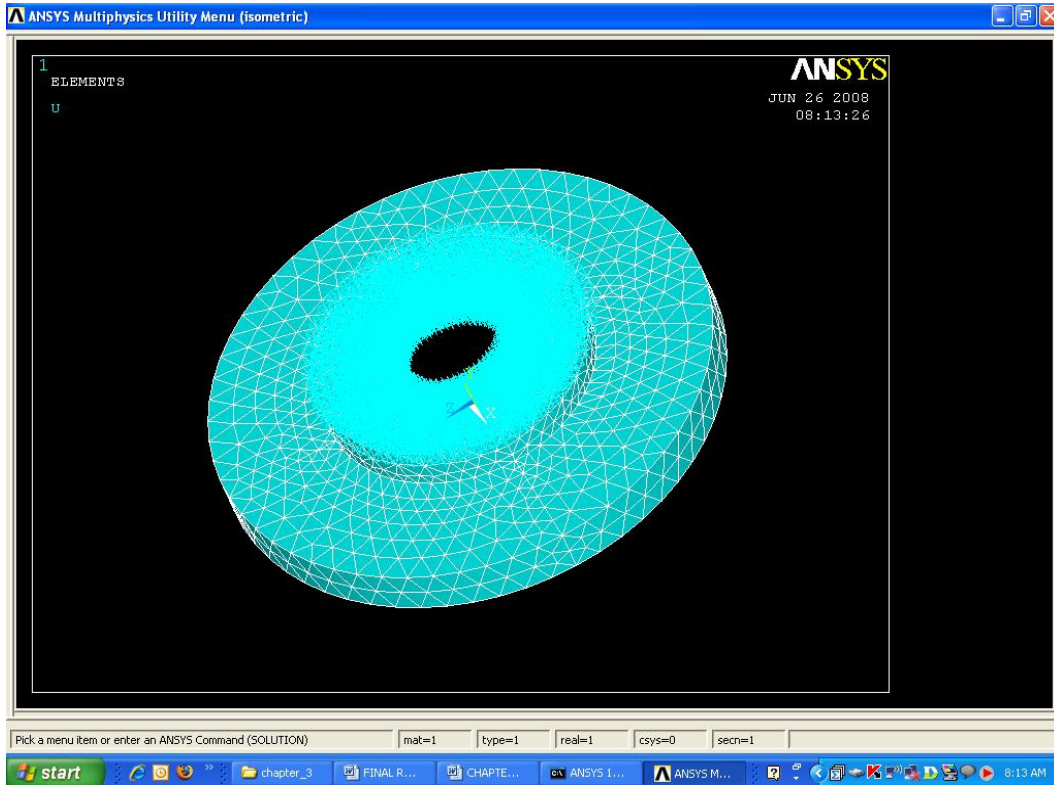


Fig 4.8 Structural model of Disk brake

## 4.8 SOLUTION

In the solution procedure, frontal solver is used. It involves

- After the individual element matrices are calculated, the solver reads in the degree of freedom (DOF) for the first element.
- The program eliminates any degrees of freedom that can be expressed in terms of the other DOF by writing an equation to the .TRI file. This process repeats for all the elements until all the degree of freedom have been eliminated and a complete triangular zed matrix is left on the .TRI file.

- The term frequently used is the frontal solver is wave front. The wave front is the number of degrees of freedom retained by the solver while triangularization of the matrix.
- The nodal solution plot of temperature distribution in thermal analysis.
- Graph of the temperature variation with respect to the radial distance from the point of application of the heat flux.
- Graph of the temperature variation with respect to the time.
- The nodal solution plot of Stress distribution in structural analysis.

# CHAPTER - 5

## RESULTS AND DISCUSSION

### 5.1 VALIDATION OF RESULTS

First of all, to validate the present method, a comparison of transient results with the steady state solution of thermo elastic behaviors was performed for the operation condition of the constant hydraulic pressure  $P = 1\text{Mpa}$  and angular velocity  $\omega = 50\text{ rad/s}$  ( drag brake application) during 10 seconds. If the transient solution for this operation condition converges to the steady solution as time elapse, it can be regarded as validation of the applied transient scheme. The thermal boundary conditions used are adiabatic on the boundary of the inner and outer radius and the prescribed temperature condition  $T = 20^\circ\text{C}$  on the both boundaries along the radius of the lower and upper pad by assumption of the cooling state. The material properties and operation conditions used for the validation of the transient thermo elastic scheme are given in Table No -5.1. The time step  $\Delta t = 0005\text{ sec.}$  was used.

Table No. - 5.1

<b>Material Properties</b>	<b>Pad and Disk</b>
Thermal conductivity, $K$ (w/m k)	50
Density, $\rho$ ( kg/m <sup>3</sup> )	1800
Specific heat , $c$ (J/Kg k)	1.88
Poisson's ratio, $\nu$	0.3
Thermal expansion , $\alpha$ ( $10^{-6} / k$ )	0.3
Elastic modulus, $E$ (GPa)	50.2
Coefficient of friction, $\mu$	0.2
<b>Operation Conditions</b>	
Angular velocity, $\omega$ (rad/s)	50
Hydraulic pressure, $P$ (Mpa)	1

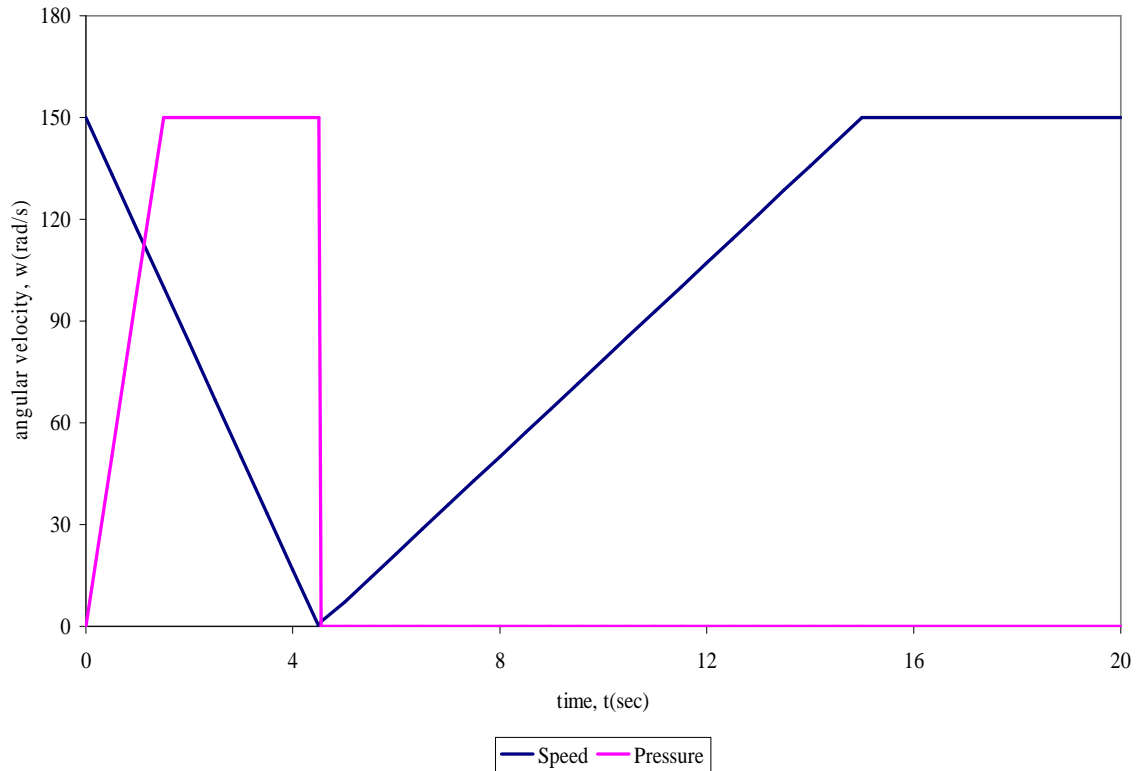


Fig 5.1 Load Curve

Fig 5.2 shows the heat flux distribution on the friction surfaces for the steady and transient (at  $t=10$  sec) solution. Actually, after time  $t=3$  sec, a change of heat flux distribution does scarcely occur, and then the steady state is reached. Also, this result indicates that the heat flux distribution on each friction surface occur dissimilarly as time elapse. The major cause of these phenomena is that the contact condition on the friction surfaces is changed to satisfy the new equilibrium state due to the rise in temperature. Fig 5.3 presents the temperature distributions on the friction surfaces for the steady and transient (at  $t=10$  sec) results. As the preceding results, the trend is for the temperature distribution to converge towards the steady state.

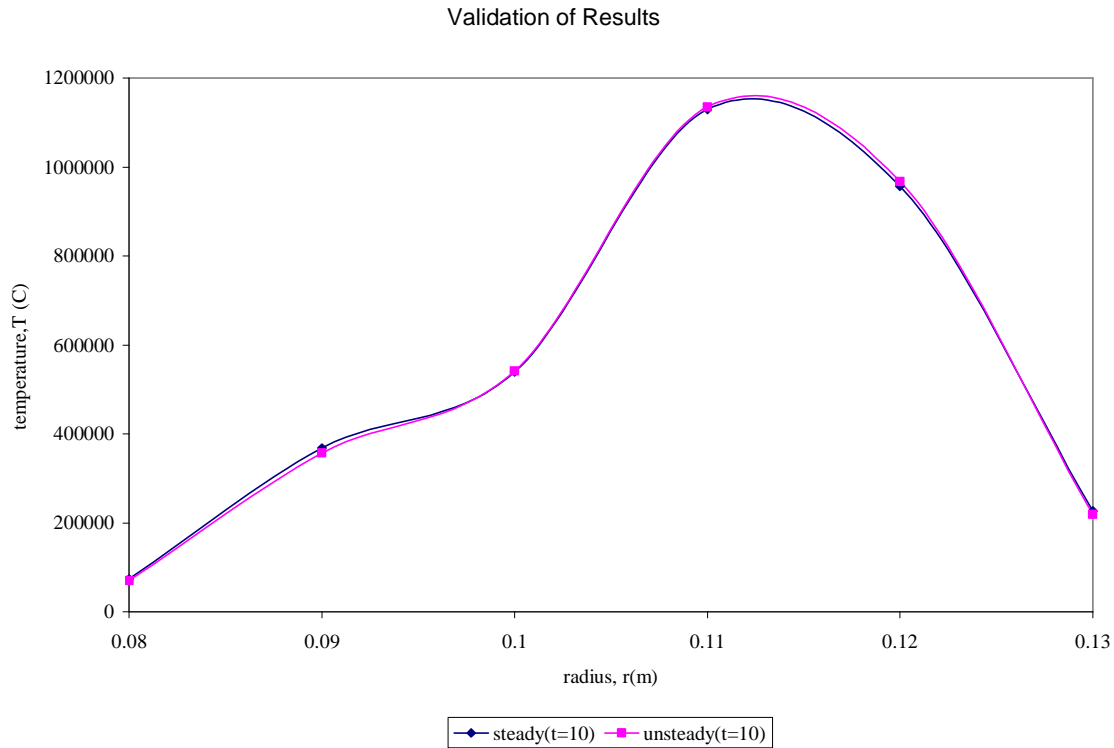


Fig. 5.2 Heat Flux distribution on friction surfaces in various braking step

## 5.2 THERMO ELASTIC BEHAVIOR IN THE REPEATED BRAKE APPLICATION

To investigate the transient thermo elastic analysis behavior of disk brake, the ANSYS simulation is obtained in 10 repeated brake applications. In actually, variation of the rotating speed during braking must be determined through vehicle dynamics. However, in this study, the rotating speed of disk was considered to be a known value. The time history of hydraulic pressure  $P_h$  and angular speed  $\omega$  assumed for brake cycle is shown in Fig 5.1. One cycle is composed of braking (4.5 sec), acceleration (10.5), and constant speed driving (5 sec). In each process, the hydraulic pressure  $P_h$  was assumed to linearly increase to 1 MPa by 1.5 sec and then kept constant until 4.5 sec. Also, the angular velocity  $\omega$  was assumed to linearly decay and finally became zero at 4.5 sec. The time step  $\Delta t = 0.001$  sec was used in the computations. The material properties adopted in the

computations are shown in Table No- 5.2. The heat convection coefficient is considered  $h = 100 \text{ (} w / m^2 k \text{)}$ .

Table No – 5.2

<b>Material Properties</b>	<b>Pad</b>	<b>Disk</b>
Thermal conductivity, K (w/m k)	5	57
Density, $\rho$ ( kg/m <sup>3</sup> )	1400	7100
Specific heat , c (J/Kg k)	1000	452
Poisson's ratio, $\nu$	0.25	0.25
Thermal expansion , $\alpha$ ( $10^{-6} / k$ )	10	11
Elastic modulus, $E$ (GPa)	1	106
Coefficient of friction, $\mu$	0.0667	
<b>Operation Conditions</b>		
Angular velocity, $\omega$ (rad/s)		150
Hydraulic pressure, $P$ (Mpa)		1

In order to obtain a clear view of the thermo elastic behaviors of the present disk brakes, the transient responses of the thermal state at various braking steps are illustrated in Fig 5.16 to 5.19. In cases of Fig 5.16 (a) – (d), the hydraulic pressure increases linearly to 1MPa and the angular velocity linearly decays from 150 rad/s (Case 1). The temperature distributions show high gradients near the region of friction surfaces and are almost symmetric about the disk's mid plane at the early steps of brake application as shown in Fig 5.17(a).

As the braking step progresses, due to the non-uniform growth of normal pressure on the friction surfaces, the distribution of temperature of disk brakes becomes non-symmetric and unstable as shown in Fig 5.17 (b)-(d). This is the phenomenon of thermo elastic instability. Fig 5.18 (a)-(d) present the results for Stainless steel disk. Unlike in the previous results in Fig 5.17 (b)-(d), the distribution of temperatures of the disk brake is almost symmetrical about the disk's mid plane and the Thermo Elastic Instability phenomenon does not occur during the braking process.

Table No- 5.3

<b>Material Properties</b>	<b>Pad</b>	<b>Disk</b>
Thermal conductivity, $K$ (w/m k)	5	17.2
Density, $\rho$ ( kg/m <sup>3</sup> )	1400	7800
Specific heat , $c$ (J/Kg k)	1000	500
Poisson's ratio, $\nu$	0.25	0.3
Thermal expansion , $\alpha$ ( $10^{-6} / k$ )	10	16
Elastic modulus, $E$ (GPa)	1	190
Coefficient of friction, $\mu$	0.0667	
<b>Operation Conditions</b>		
Angular velocity, $\omega$ (rad/s)		150
Hydraulic pressure, $P$ (Mpa)		1

Validation of Results

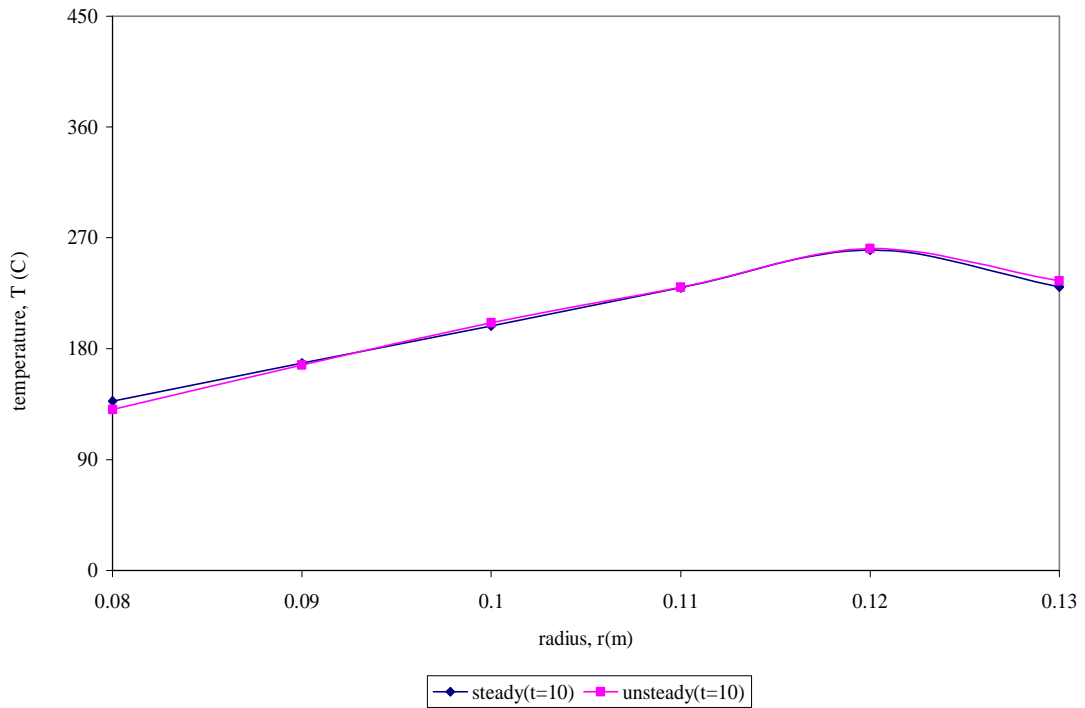


Fig. 5.3 Temperature distribution on friction surfaces in various braking step

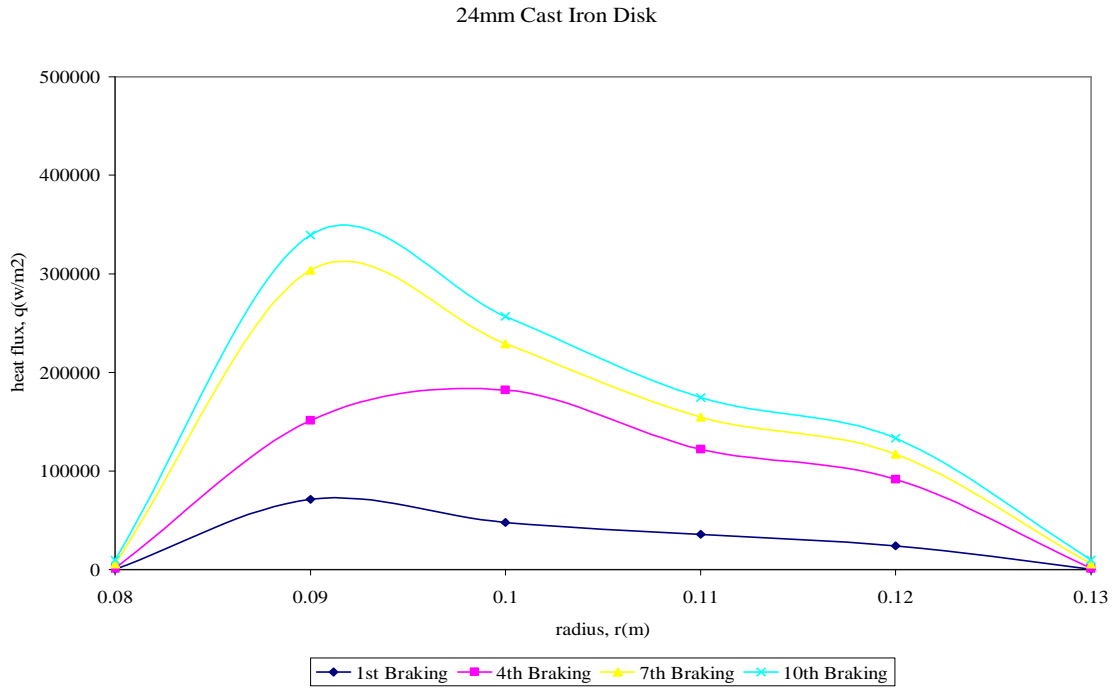


Fig. 5.4 Heat Flux distribution on friction surfaces in various braking step

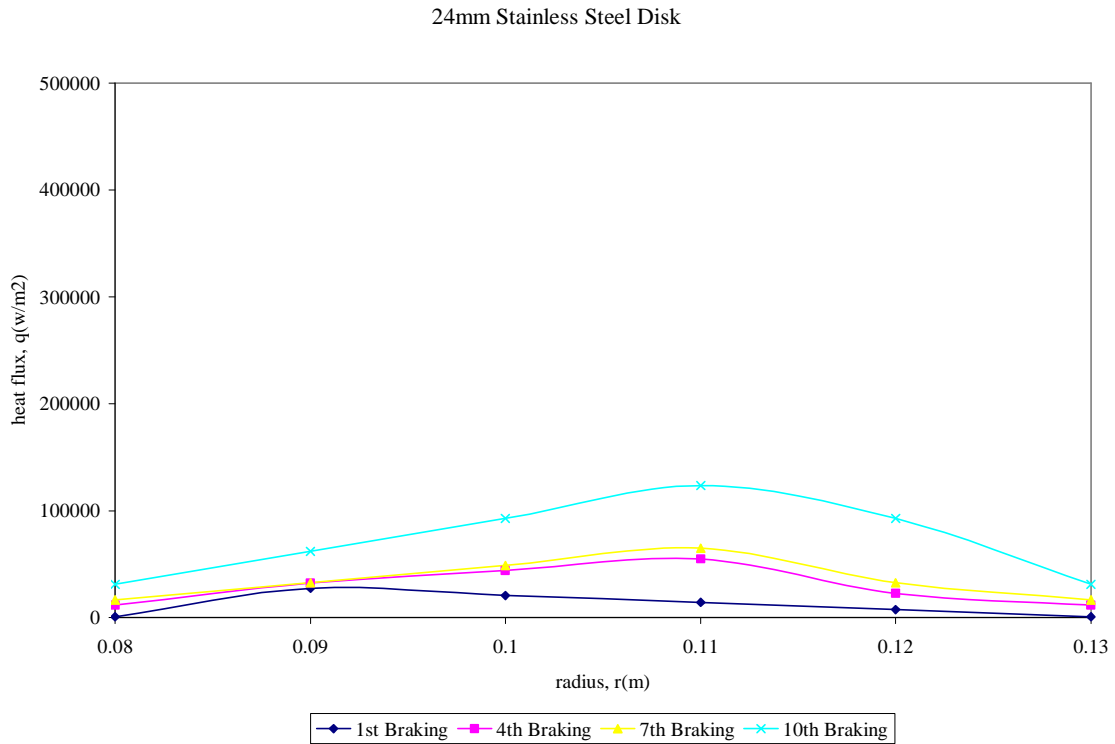


Fig. 5.5 Heat Flux distribution on friction surfaces in various braking step

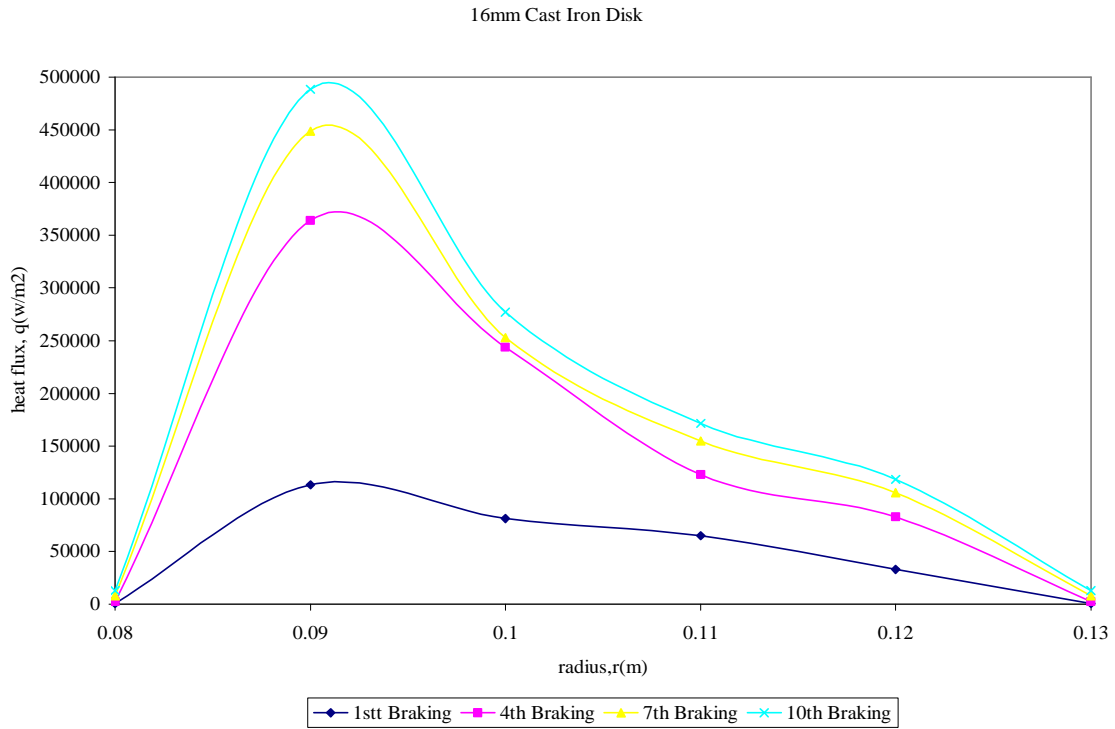


Fig. 5.6 Heat Flux distribution on friction surfaces in various braking step

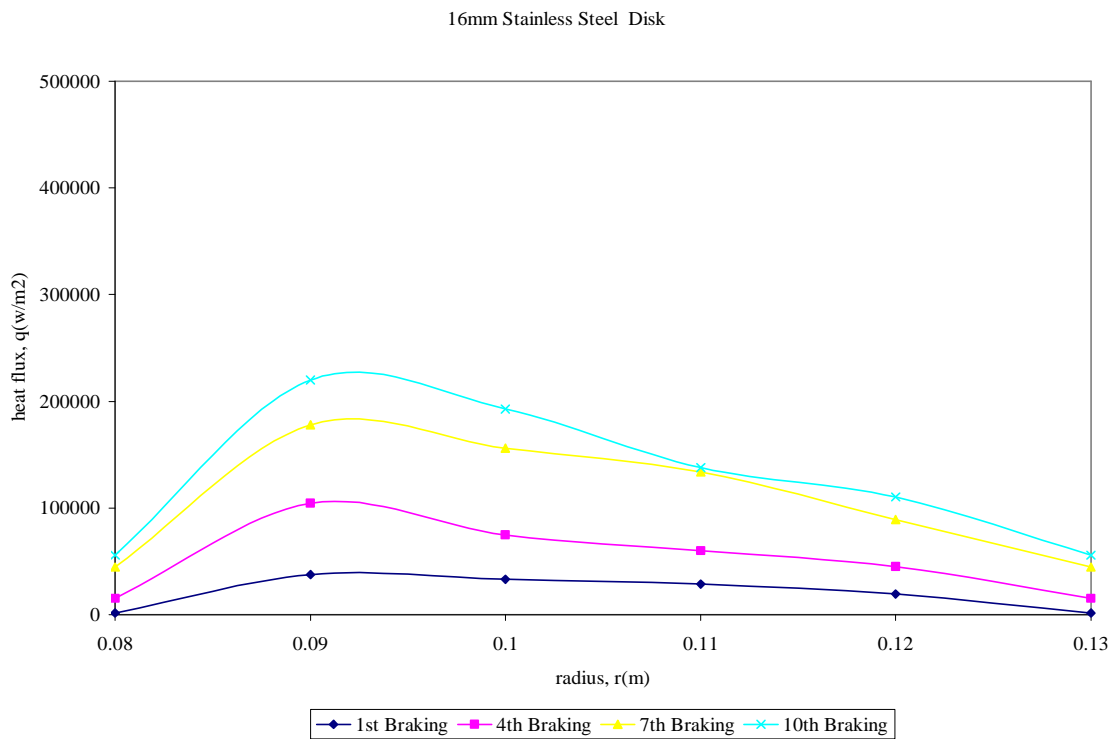


Fig 5.7 Heat Flux distribution on friction surfaces in various braking step

In addition to the TEI phenomenon of disk brakes, the influence of the material properties of the pad on the contact ratio of friction surfaces is considered to facilitate better conceptual design of the disk brake system. Fig 5.8 and Fig 5.9 showed the effect of material properties in a thermo elastic contact stability problem with one body in contact with a rigid plane surface. However, the present results in Fig 5.8 and Fig 5.10 are further show the relative importance of each parameter on the variation of thermo elastic behaviors. The thermal expansion coefficient and the elastic modulus of pad materials have a larger effect on the thermo elastic behaviors of disk brakes. In particular, when the elastic modulus of pad material is halved, all friction surfaces between the disk and pad are in perfect contact for all of the braking steps. Therefore, the softer pad improves the contact pressure distribution and results in a more even temperature distribution.

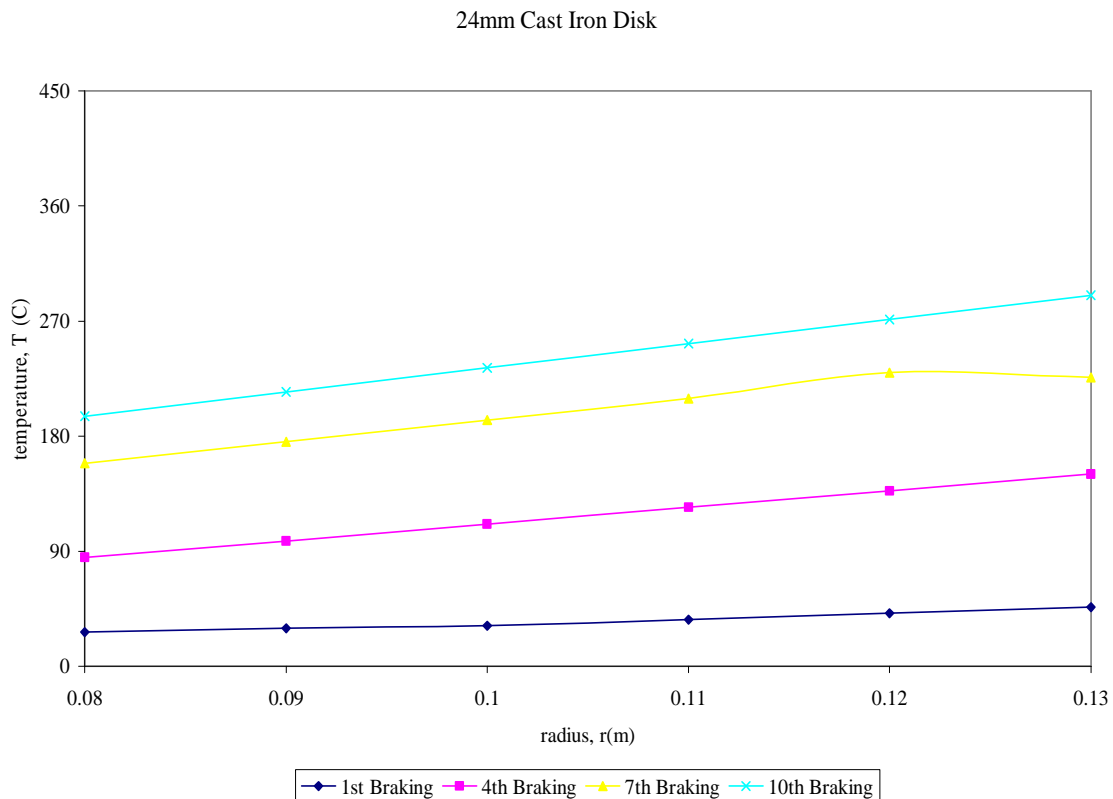


Fig. 5.8 Temperature distribution on friction surfaces in various braking step

Also, similar analyses were carried to investigate the effects of disk material properties. It was found that the thermal expansion coefficient and the specific heat of disk materials have a larger influence on the thermo elastic behaviors. Based on these numerical results, the thermo elastic behaviors of the carbon–carbon composite disk brake are also investigated. Carbon–carbon composites are extensively used as aircraft disk brakes, rocket re-entry nose tips, and high speed railway brakes on account of their excellent material properties (high temperature resistance, low density, high thermal conductivity and heat capacity, and low thermal expansion). In this section, the transient thermo elastic analysis of the carbon–carbon composite disk brake is performed for the drag brake application ( $P_h = 1\text{MPa}$ ,  $\omega = 100\text{ rad/s}$ ) for 10 s, and then the results in the case of carbon–carbon composites (orthotropic case) are compared with those using the material properties listed in Table 5.2 (isotropic case). The material properties of carbon–carbon composites used in the computations are presented in Table 5.4.

Table No – 5.4

<b>Material Properties</b>	<b>Pad and Disk</b>
Thermal conductivity, $K_r$ (w/m k)	50
Thermal conductivity, $K_z$ (w/m k)	10
Density, $\rho$ ( kg/m <sup>3</sup> )	1800
Specific heat , c(J/Kg k)	1420
Poisson's ratio, $\nu_{r\theta}$	0.3
Poisson's ratio, $\nu_{rz}$	0.33
Thermal expansion , $\alpha_r$ ( $10^{-6} / k$ )	0.31
Thermal expansion , $\alpha_z$ ( $10^{-6} / k$ )	0.29
Elastic modulus, $E_r$ (GPa)	50.2
Elastic modulus, $E_z$ (GPa)	5.89
Shear modulus, $G_{rz}$ (GPa)	2.46
Coefficient of friction, $\mu$	0.0667
Angular velocity, $\omega$ (rad/s)	100

24mm Stainless Steel

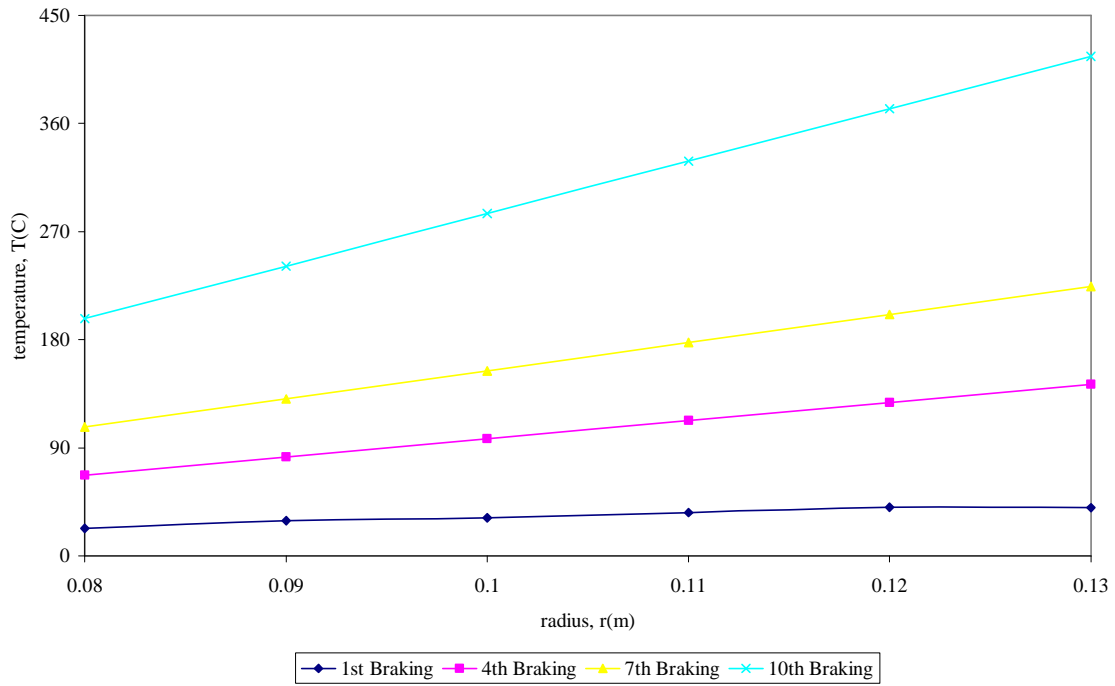


Fig. 5.9 Temperature distribution on friction surfaces in various braking step

16mm Cast Iron Disk

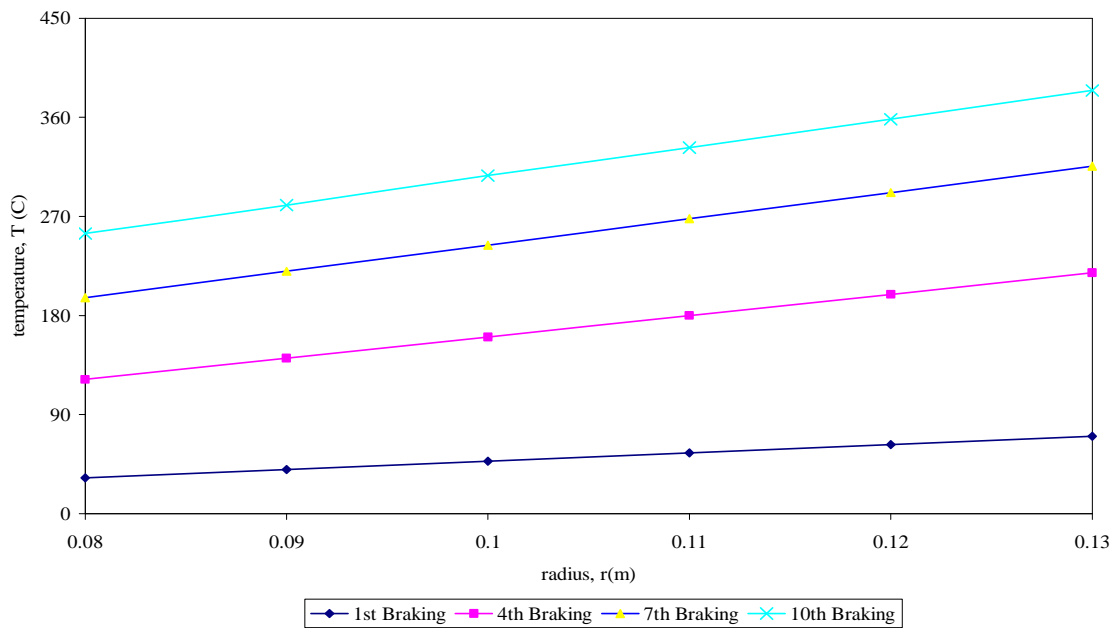


Fig. 5.10 Temperature distribution on friction surfaces in various braking step

### 16mm Stainless Steel Disk

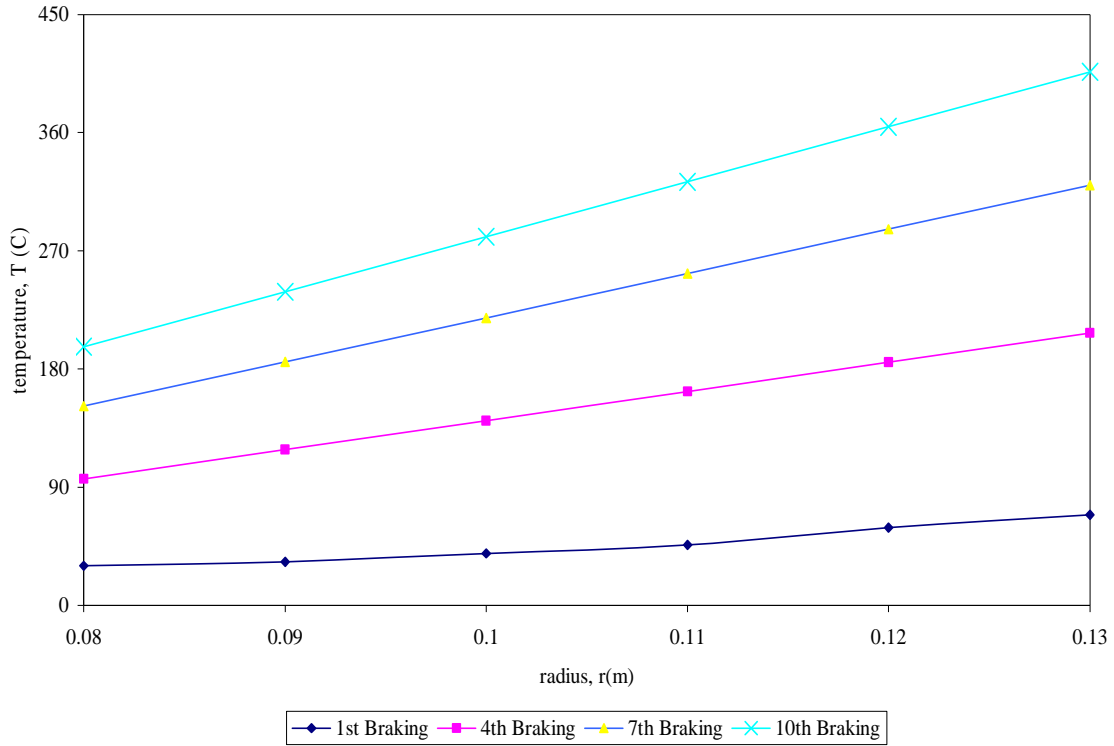


Fig. 5.11 Temperature distribution on friction surfaces in various braking step

Fig 5.12, 5.13, 5.14 and 5.15 show the heat flux and temperature distributions on the friction surfaces at time  $t = 1$  and  $10$  s for the isotropic and orthotropic material respectively. Compared with the isotropic case, the heat flux of the orthotropic one are very uniformly distributed along the friction surfaces and results in a more even temperature distribution, namely, a thermo elastic stable state. These results show that the disk brakes made of isotropic material can provide better braking performance than the orthotropic metal ones.

Isotropic, 24mm Disk

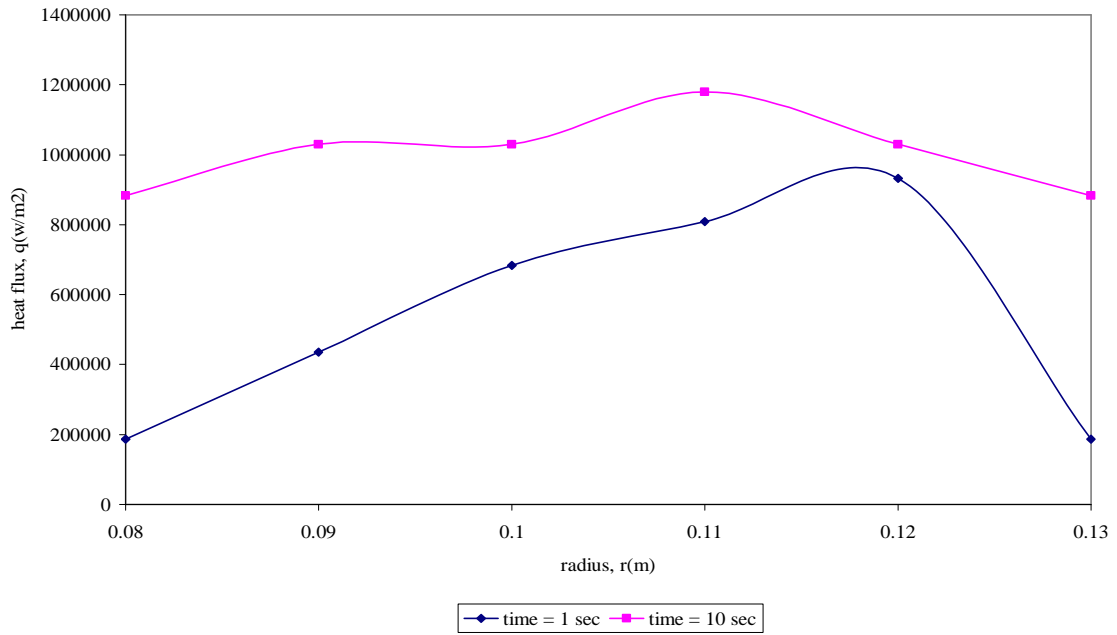


Fig. 5.12 Heat Flux distribution on friction surfaces in various braking step

Orthotropic, 24mm Disk

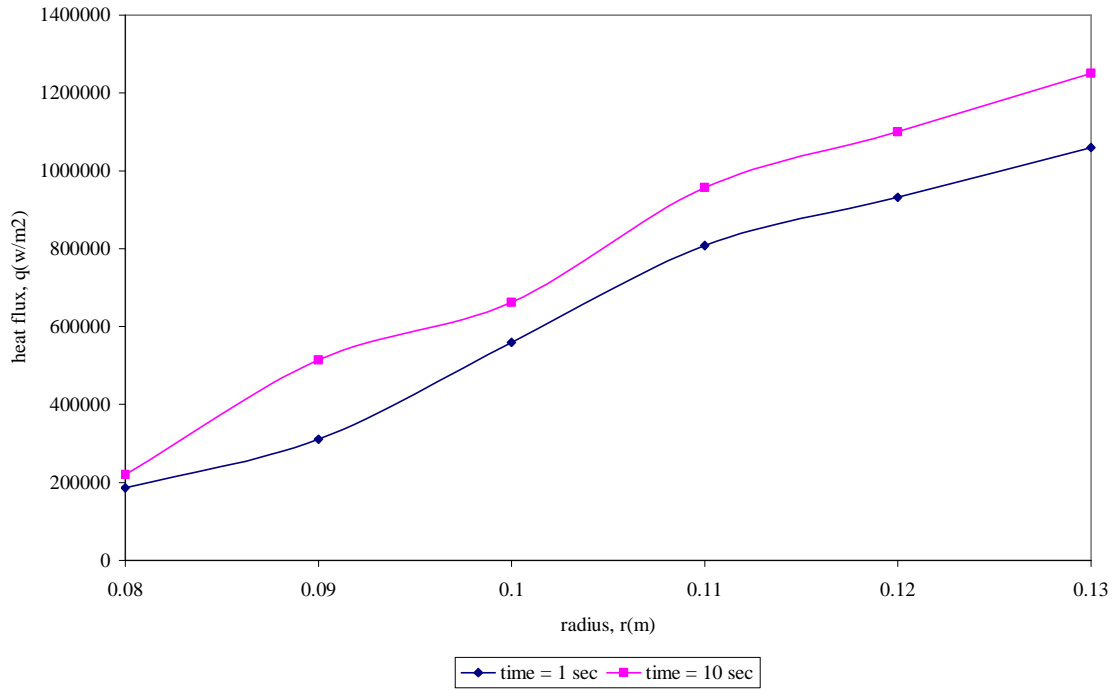


Fig. 5.13 Heat Flux distribution on friction surfaces in various braking step

Isotropic ,24mm Disk

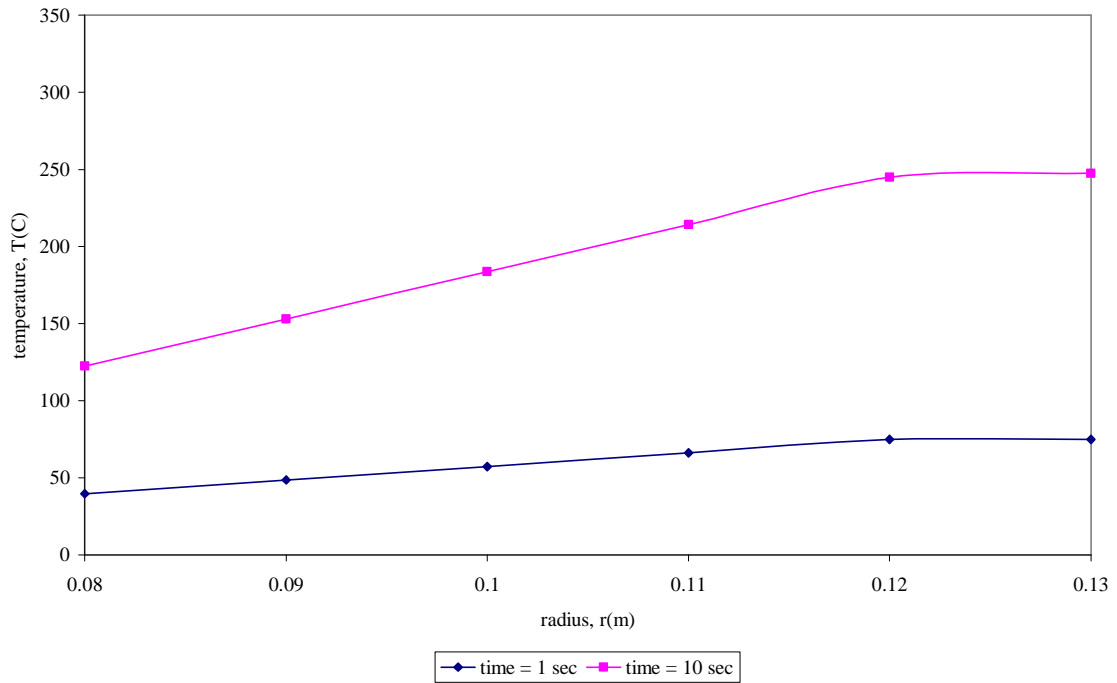


Fig. 5.14 Temperature distribution on friction surfaces in various braking step

Orthotropic, 24mm Disk

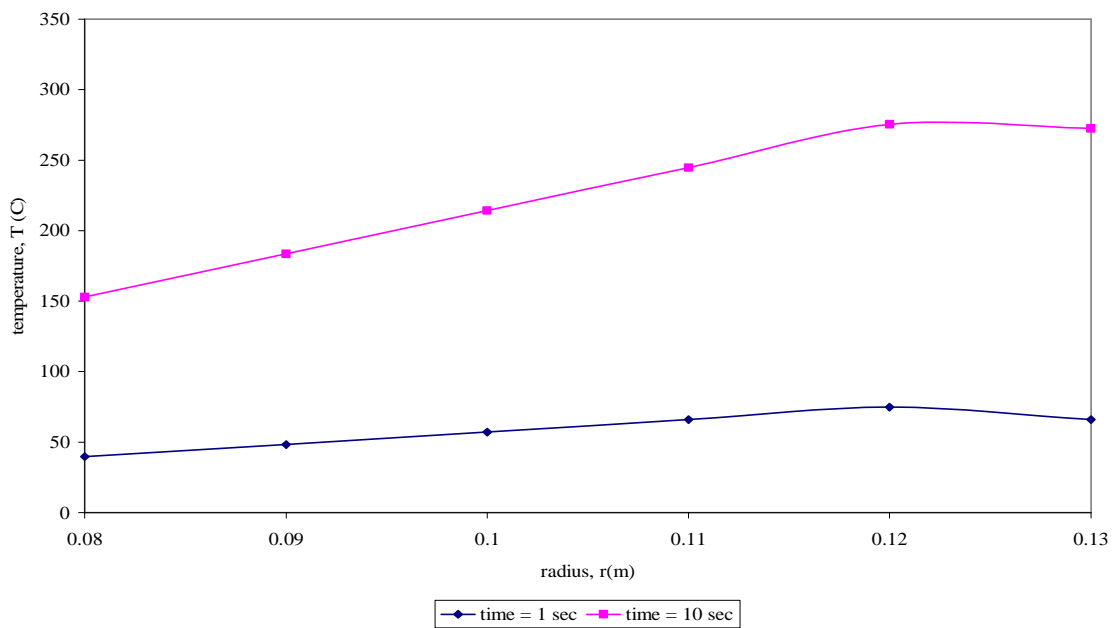


Fig. 5.15 Temperature distribution on friction surfaces in various braking step

Fig 5.16 shows the temperature distribution on various friction surfaces in various braking steps, i.e. 1<sup>st</sup> braking to 10<sup>th</sup> braking. As shown in Fig 5.16, the maximum temperature rise after 10<sup>th</sup> braking step in Stainless Steel disk of 24mm flange width is 415.83 °C . But the corresponding thermal stresses induced at this temperature are 56.1 MPa (Hoop Stress) .And maximum temperatures after 10<sup>TH</sup> braking step in Cast iron disk of 14mm flange width is 290.38°C .But. But the corresponding thermal stresses induced at this temperature are 56.7 MPa (Hoop Stress), as shown in Fig 5.20. From above discussed two cases, we can conclude that Cast Iron of flange width of 24mm disk is best suitable for braking application, but we also analyzed another disk of 16mm of same material for the same application. We found that the maximum temperature rise in Cast Iron disk after 10<sup>th</sup> braking step is 384.33 °C , as shown in Fig 5.16, which is less than the maximum temperature rise in Stainless Steel (406.49 °C ). The thermal stresses induced at 384.33 °C in Cast Iron disk (16mm) is 8.58 Mpa, (Hoop Stresses),as shown in Fig 5.26, which is with in safe limit and less than the thermal stresses induced in all disk after 10<sup>th</sup> braking step. So we say finally cast Iron disk of 16mm flange width is best suitable for the above said braking application.

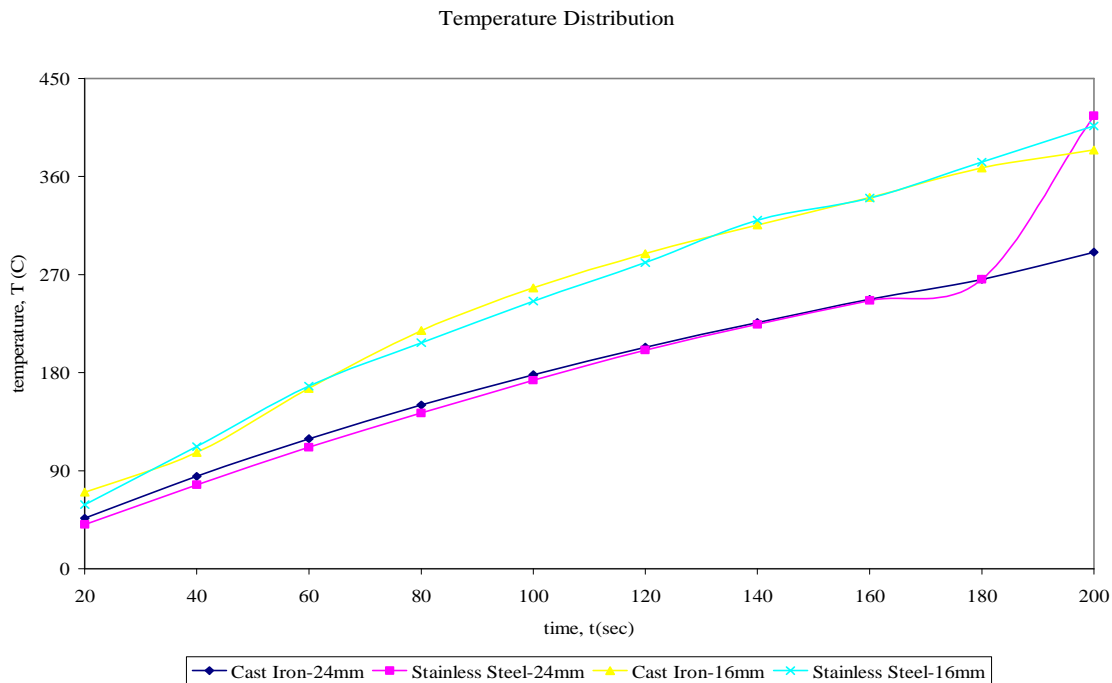
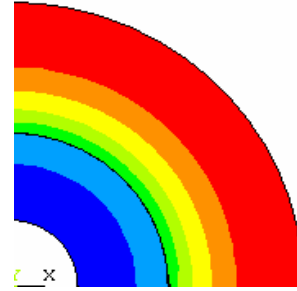


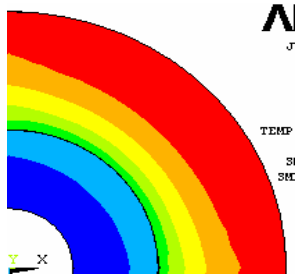
Fig. 5.16 Temperature distribution on friction surfaces in various braking step



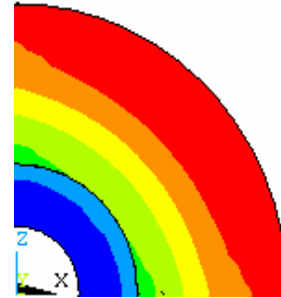
(a) 1<sup>st</sup> braking



(b) 4<sup>th</sup> braking



(c) 7<sup>th</sup> braking



(d) 10<sup>th</sup> braking

Fig 5.17 Temperature contours of 24mm Cast Iron disk (a)-(d)



(a) 1<sup>st</sup> braking



(b) 4<sup>th</sup> braking



(c) 7<sup>th</sup> braking



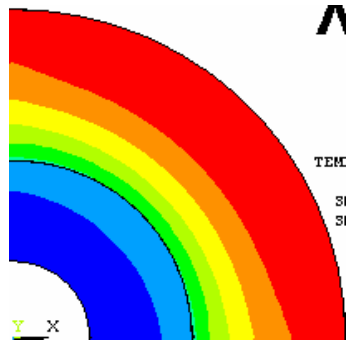
(d) 10<sup>th</sup> braking

Fig 5.18 Temperature contours of 24mm stainless steel disk (a)-(d)

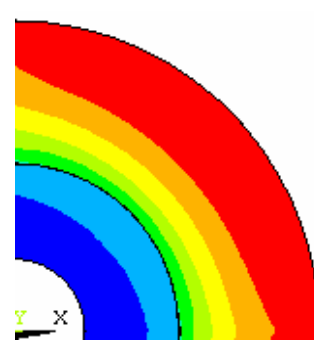


(a) 1<sup>st</sup> braking

(b) 4<sup>th</sup> braking

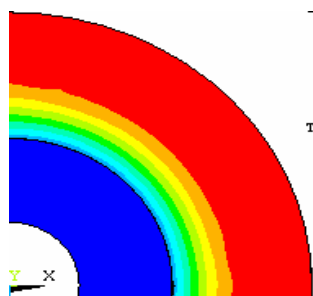


(c) 7<sup>th</sup> braking

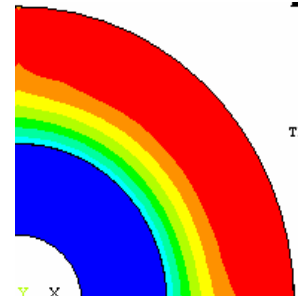


(d) 10<sup>th</sup> braking

Fig 5.19 Temperature contours of 16mm Cast Iron disk (a)-(d)



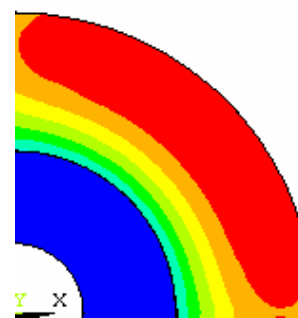
(a) 1<sup>st</sup> braking



(b) 4<sup>th</sup> braking



(c) 7<sup>th</sup> braking



(d) 10<sup>th</sup> braking

Fig 5.20 Temperature contours of 16mm Stainless Steel disk (a)-(d)

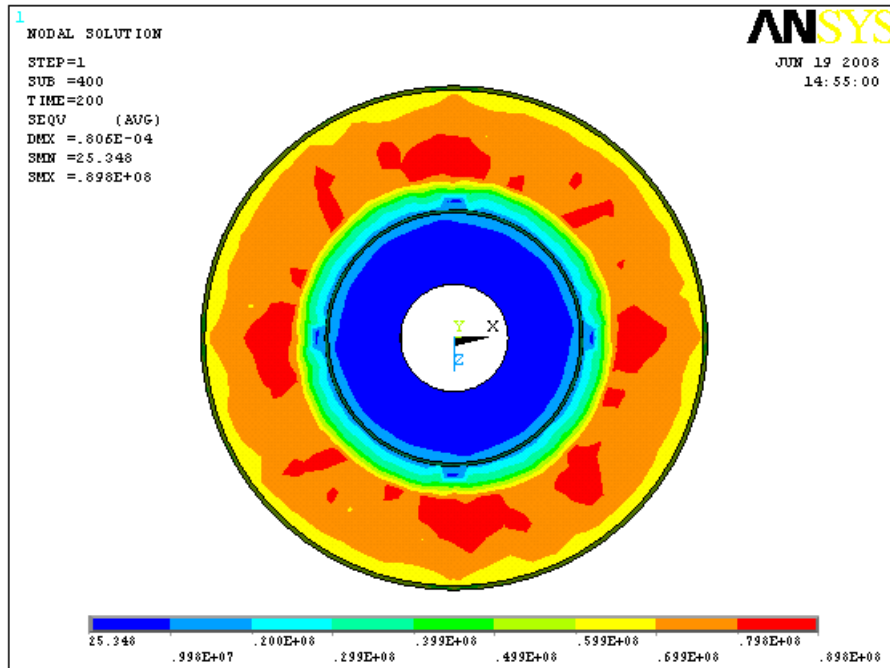


Fig 5.21 Distribution of Von misses Stress in 24 mm Cast iron Disk

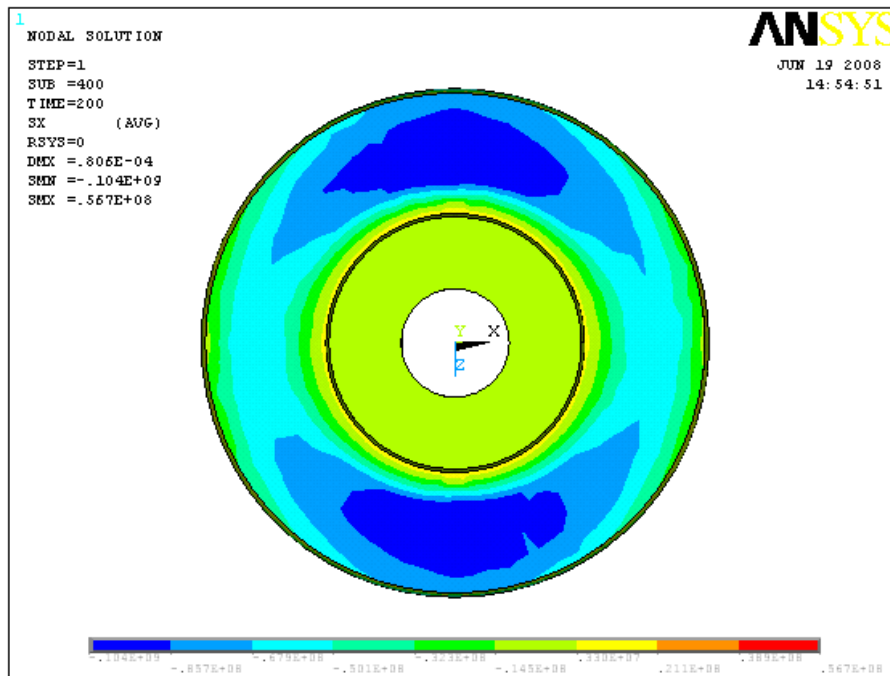


Fig 5.22 Distribution of Hoop Stress in 24 mm Cast iron Disk

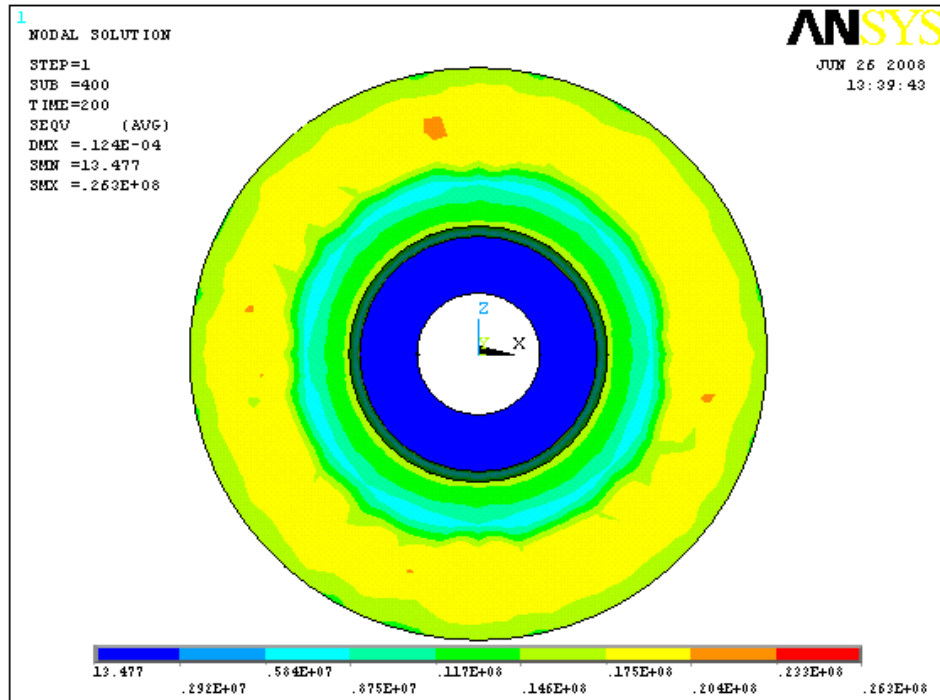


Fig 5.23 Distribution of Von misses Stress in 24 mm Stainless Steel Disk

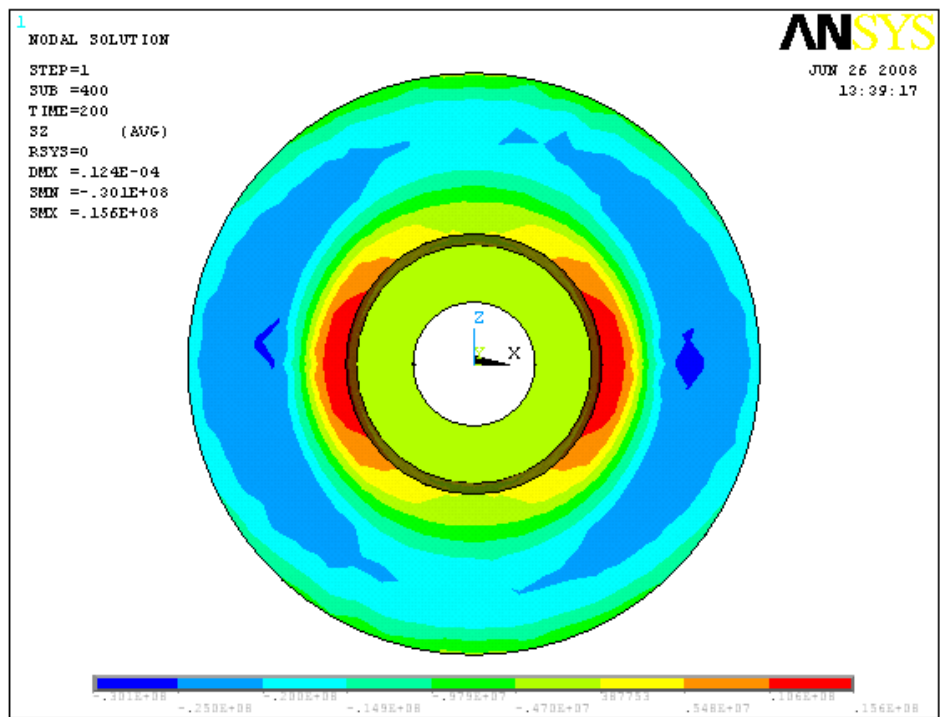


Fig 5.24 Distribution of Hoop Stress in 24 mm Stainless Steel Disk

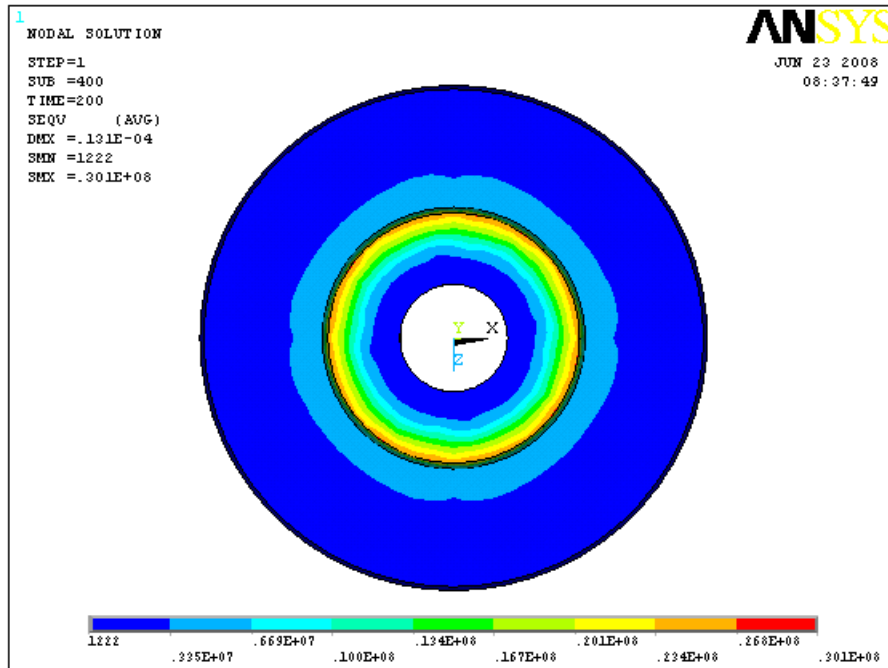


Fig 5.25 Distribution of Von misses Stress in 16 mm Cast iron Disk

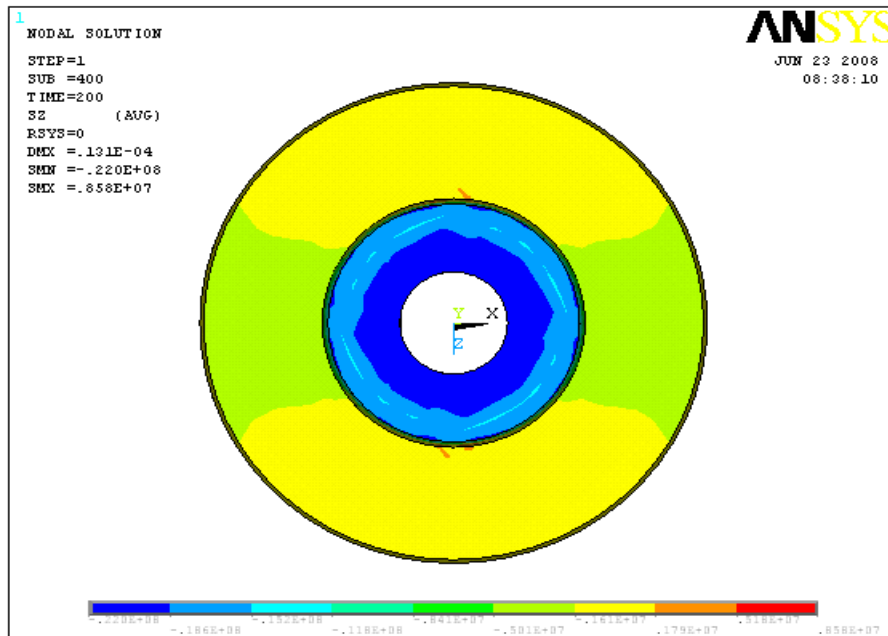


Fig 5.26 Distribution of Hoop Stress in 16 mm Cast iron Disk

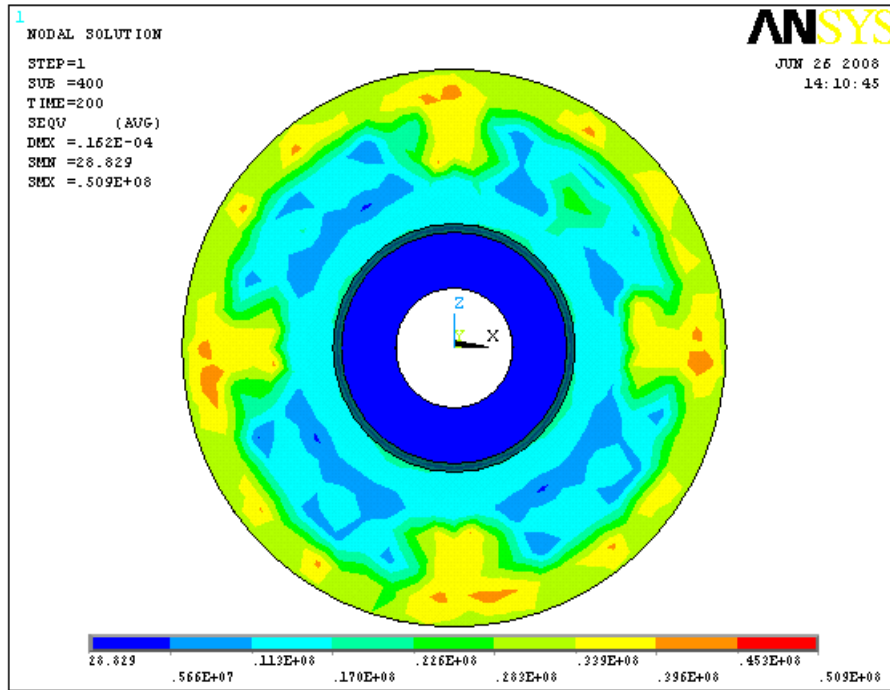


Fig 5.27 Distribution of Von misses Stress in 16 mm Stainless Steel Disk

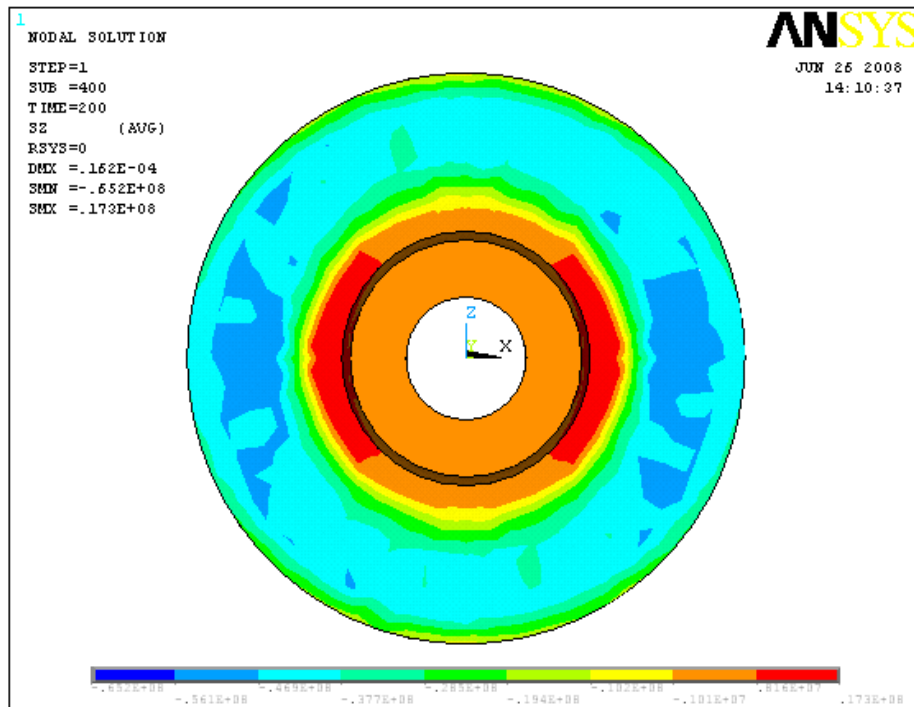


Fig 5.28 Distribution of Hoop Stress in 16 mm Stainless Steel Disk

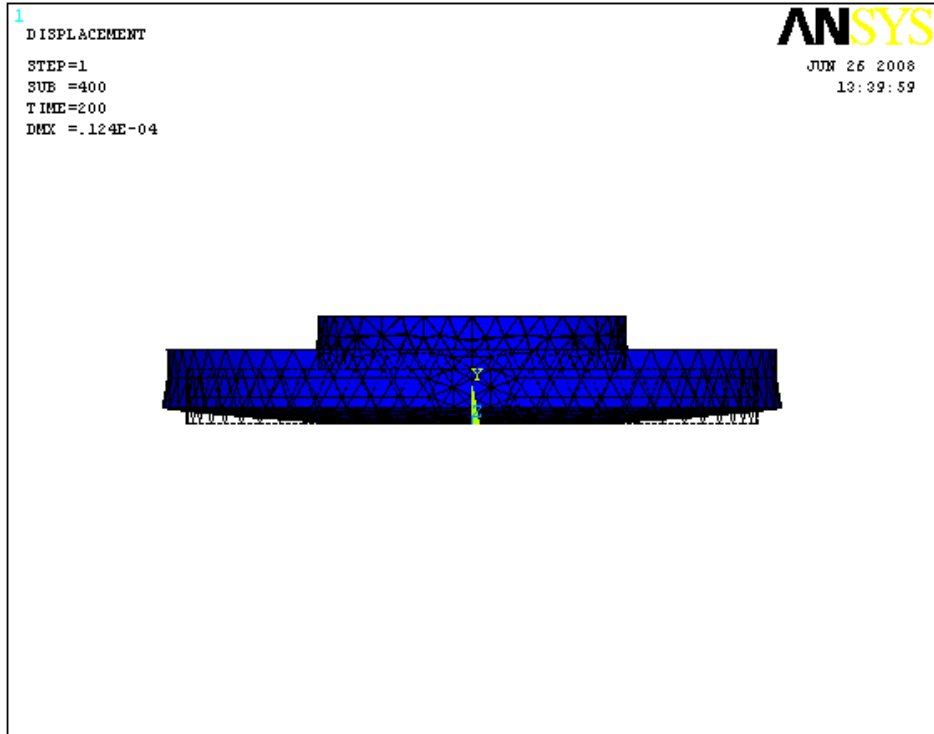


Fig 5.29 Average displacement in 24mm Cast Iron Disk

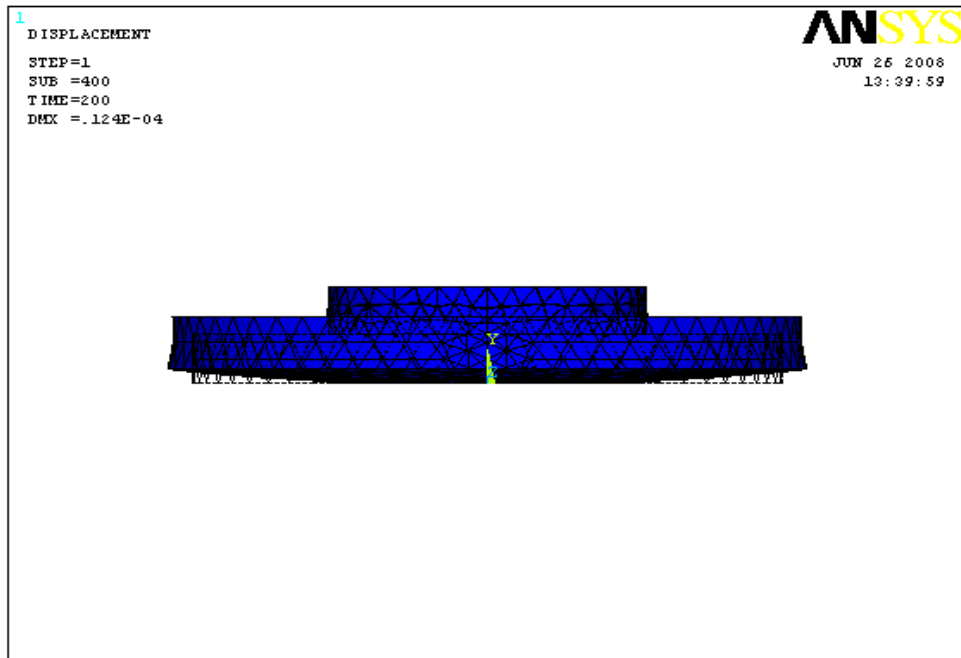


Fig 5.30 Average displacement in 24mm Stainless Steel Disk

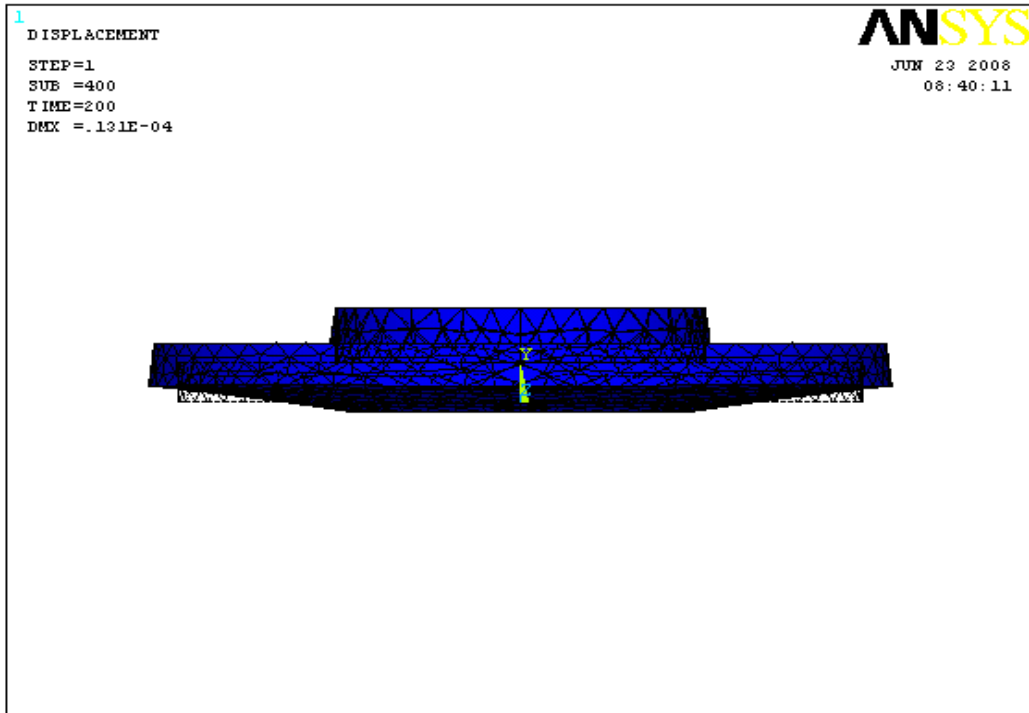


Fig 5.31 Average displacement in 16mm Cast Iron Disk

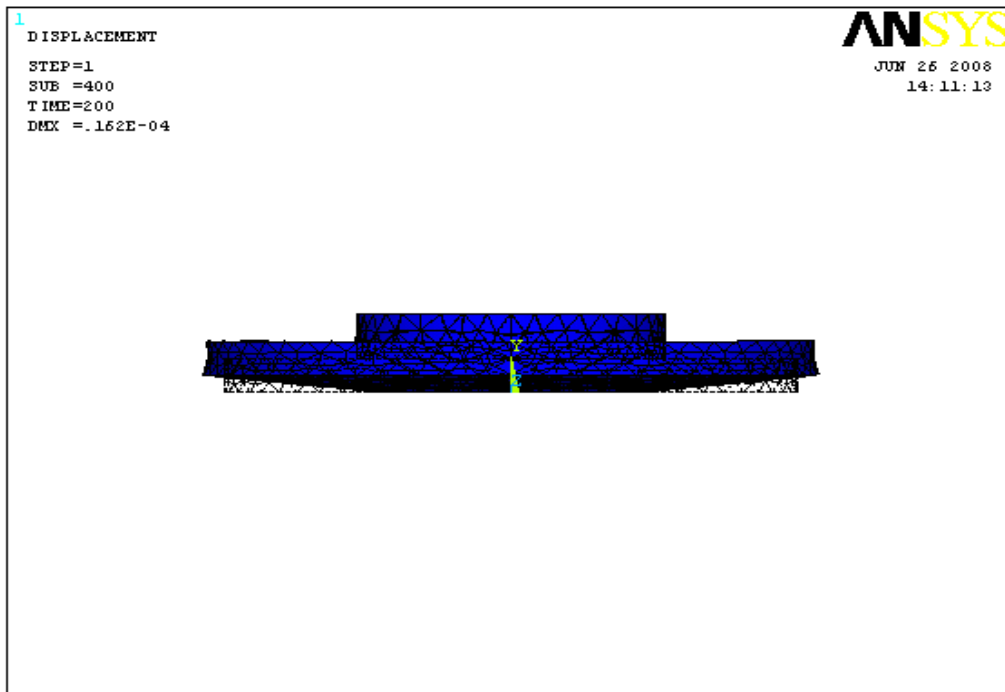


Fig 5.32 Average displacement in 16mm Stainless Steel Disk

## CONCLUSIONS

In this paper, the transient thermo elastic analysis of disk brakes in repeated brake applications has been performed. ANSYS software is applied to the thermo elastic contact problem with frictional heat generation. To obtain the simulation of thermo elastic behavior appearing in disk brakes, the coupled heat conduction and elastic equations are solved with contact problems. Also, the fully implicit scheme is used to improve the accuracy of computations in the transient analysis. Through the axis symmetric disk brake model, the TEI phenomenon on each of the friction surfaces between the contacting bodies has been investigated. The hoop stress component in disk brakes has the largest compressive stress value and must be considered as a dominant stress component from the viewpoint of stress failure. The effects of the friction material properties on the contact ratio of friction surfaces are examined and the larger influential properties are found to be the thermal expansion coefficient and the elastic modulus. Based on these numerical results, the thermo elastic behaviors of the carbon–carbon composite disk brakes are also investigated. It is observed that the isotropic disk brakes can provide better brake performance than the isotropic ones because of uniform and mild pressure distributions.

The present study can provide a useful design tool and improve the brake performance of disk brake system. From Table 6.1 we can say that all the values obtained from the analysis are less than their allowable values. Hence the brake disk design is safe based on the strength and rigidity criteria.

Comparing the different results obtained from analysis in table 6.1. It is concluded that disk brake with 16mm flange width and of material Cast Iron is the best possible combination for the present application.

Table No – 6.1

S.No	Material	Flange width (mm)	Max. Temp °C	Deflection in (mm)	Von misses stress (MPa)		Hoop Stress (MPa)	
					Max.	Min.	Max.	Min.
1	Cast Iron	24	290.38	0.0806	89.8	25e-06	56.7	-104
2	Stainless Steel	24	415.83	0.0124	26.30	-61.0	15.60	0.544
3	Cast Iron	16	384.33	0.0131	30.10	1.2e-03	8.58	-22.0
4	Stainless Steel	16	406.49	0.0162	50.90	5.66	17.30	-65.4

## **SCOPE FOR THE FURTHER STUDY**

In the present investigation of thermal analysis of disk brake, a simplified disk brake without any vents, with only ambient air-cooling is analyzed by FEM package ANSYS.

As future work, a complicated model of ventilated disk brake can be taken and there by forced convection to be considered in the analysis. The analysis still becomes complicated by considering variable thermal conductivity, variable specific heat and non uniform deceleration of vehicle. This can be considered for the future work.

## REFERENCES

1. KENNEDY, F. E., COLIN, F. FLOQUET, A. AND GLOVSKY, R. Improved Techniques for Finite Element Analysis of Sliding Surface Temperatures. Westbury House page 138-150, (1984).
2. LIN , J. -Y. AND CHEN, H. -T. Radial Axis symmetric Transient Heat Conduction in Composite Hollow Cylinders with Variable Thermal Conductivity, vol. 10, page 2- 33, (1992).
3. BRILLA, J. Laplace Transform and New Mathematical Theory of Visco elasticity, vol. 32, page 187- 195, (1997).
4. TSINOPOULOS, S. V, AGNANTIARIS, J. P. AND POLYZOS, D. An Advanced Boundary Element/Fast Fourier Transform Axis symmetric Formulation for Acoustic Radiation and Wave Scattering Problems, J.ACOUST. SOC. AMER., vol 105, page 1517-1526, (1999).
5. WANG, H. -C. AND BANERJEE, P. K.. Generalized Axis symmetric Elastodynamic Analysis by Boundary Element Method, vol. 30, page 115-131, (1990).
6. FLOQUET, A. AND DUBOURG, M.-C. Non axis symmetric effects for three dimensional Analyses of a Brake, ASME J. Tribology, vol. 116, page 401-407, (1994).
7. BURTON, R. A. Thermal Deformation in Frictionally Heated Contact, Wear, vol. 59, page 1- 20, (1980).
8. ANDERSON, A. E. AND KNAPP, R. A. Hot Spotting in Automotive Friction System Wear, vol. 135, page 319-337, (1990).
9. COMNINOU, M. AND DUNDURS, J. On the Barber Boundary Conditions for Thermo elastic Contact, ASME J, vol. 46, page 849-853, (1979).
10. BARBER, J. R. Contact Problems Involving a Cooled Punch, J. Elasticity, vol. 8, page 409- 423, (1978).

11. BARBER, J. R. Stability of Thermo elastic Contact, Proc. International Conference on Tribology, p Institute of Mechanical Engineers, page. 981-986, (1987).
12. DOW, T. A. AND BURTON, R. A. Thermo elastic Instability of Sliding Contact in the absence of Wear, *Wear*, vol. 19, page 315-328, (1972).
13. LEE, K. AND BARBER, J.R. Frictionally-Excited Thermo elastic Instability in Automotive Disk Brakes, *ASME J. Tribology*, vol. 115, page 607-614, (1993).
14. LEE, K. AND BARBER, J. R. An Experimental Investigation of Frictionally-excited Thermo elastic Instability in Automotive Disk Brakes under a Drag Brake Application, *ASME J. Tribology*, vol. 116,page 409-414, (1994).
15. LEE, K. AND BARBER, J. R. Effect of Intermittent Contact on the Stability of Thermo elastic Contact, *ASME J. Tribology*, vol. 198, page 27- 32, (1995).
16. ZAGRODZKE, S, BARBER, J. R. AND HULBERT, G.M. Finite Element Analysis of Frictionally Excited Thermo elastic Instability, *J. Thermal Stresses*, vol. 20, page 185-201, (1997).
17. LEROY, J. M., FLOQUET, A. AND VILLECHAISE, B. Thermo-mechanical Behavior of Multilayered Media: Theory, *ASME J. Tribology*, vol. 111, page 530-544, (1989).
18. GONSKA, H. W. AND KOLBINGER, H. J. Temperature and Deformation Calculation of Passenger Car Brake Disks, Proc. ABAQUS User's Conference, Aachen, Germany, page 21- 232, (1993).
19. AKIN, J. E. Application and Implementation of Finite Element Methods, Academic Press, Orlando, FL, page 318-323, (1982).
20. ZAGRODZKI, P. Analysis of thermo mechanical phenomena in multi disk clutches and brakes, *Wear* 140, page 291-308, (1990).
21. COOK, R. D. Concept and Applications of Finite Element Analysis, Wiley, Canada, (1981).
22. ZIENKIEWICZ, O. C. The Finite Element method, McGraw-Hill, New York, (1977).
23. BEEKER, A.A. The Boundary Element Method in Engineering, McGraw-Hill, New York, (1992).